chemosensors

MDPI

Review

Recent Advances and Perspectives Regarding Paper-Based Sensors for Salivary Biomarker Detection

Cong Chen [1], Lulu Tian [1], Wen Li [1], Kun Wang [1], Qijing Yang [1], Jinying Lin [1], Tianshou Zhang [1,*], Biao Dong [2,*] and Lin Wang [1,*]

[1] Department of Oral Implantology, School and Hospital of Stomatology, Jilin University, Changchun 130021, China; chencong21@mails.jlu.edu.cn (C.C.); tianll22@mails.jlu.edu.cn (L.T.); lwen22@mails.jlu.edu.cn (W.L.)

[2] State Key Laboratory on Integrated Optoelectronics, College of Electronic Science and Engineering, Jilin University, Changchun 130021, China

* Correspondence: zhangts1213@jlu.edu.cn (T.Z.); dongb@jlu.edu.cn (B.D.); wanglin1982@jlu.edu.cn (L.W.)

Abstract: Paper-based sensors overcome the drawbacks of conventional sensors in terms of their flexibility, portability, and stability compared to conventional sensors. Moreover, as a noninvasive bodily fluid, saliva contains various biomarkers related to physical status, which makes it perfectly matched with to use of paper-based sensors to manufacture a convenient and inexpensive disposable sensing device. This review focuses on the recent advances and progress in the design of paper-based salivary sensors and their applications. The first part mainly discusses various paper-based sensors and their advanced compositions, including dipstick assay, lateral flow assay, and microfluidic analytical device. Different detection methods in salivary biomarker detection are specially introduced in the secondary section, then their multiple potential applications and prospects are summarized. The sensor has excellent advantages for saliva detection, provides a reliable platform for point-of-care tests and telemedicine, and epically promotes the development of the medical Internet of Things.

Keywords: paper-based sensor; saliva biomarker; point of care

Citation: Chen, C.; Tian, L.; Li, W.; Wang, K.; Yang, Q.; Lin, J.; Zhang, T.; Dong, B.; Wang, L. Recent Advances and Perspectives Regarding Paper-Based Sensors for Salivary Biomarker Detection. *Chemosensors* **2023**, *11*, 383. https://doi.org/10.3390/chemosensors11070383

Academic Editor: Camelia Bala

Received: 10 May 2023
Revised: 29 June 2023
Accepted: 4 July 2023
Published: 7 July 2023

1. Introduction

Medical advances in technology and facilities have reduced the overall mortality and morbidity linked to some human diseases in the past decades. However, many diseases still pose severe threats to human health. Historically difficult-to-treat diseases such as cancer and HIV are still searching for the best treatment options. The statistics show that about 600 thousand people in the United States will die from cancer in 2022, equivalent to nearly 1700 deaths per day [1]. Additionally, there is a growing concern about chronic systemic diseases such as cardiovascular, diabetes, and hypertension, especially in the elderly population, and will become increasingly prominent at the advent of the population health aging trend [2]. At the same time, coronavirus disease 2019 (COVID-19) has rapidly emerged worldwide since 2019. Until January 2023, more than 700 million confirmed COVID-19 cases [3]. Therefore, disease diagnosis, prevention, and treatment remain essential prerequisites for improving quality of life. In recent years, the evolving knowledge of the disease has made physicians shift the focus of therapy to prevention. However, diagnosis is often based on clinical experience, especially in some remote areas where laboratory conditions are not available. Meanwhile, prevention measures usually have geographic disparities. If diseases or morbidity trends can be diagnosed using a simple and inexpensive diagnostic method, it will significantly improve the level of treatment. Therefore, developing a class of simple and affordable diagnostic and monitoring devices is necessary.

To cater to the sample's high sensitivity and low detection limits, most analytical methods require expensive equipment, which relies on a high standard of professional

quality for testing conditions and inspectors. However, inexpensive, rapid, and efficient in situ detection and monitoring technologies are gradually needed to provide more information regarding real-time physical situations or the extent and magnitude of the disease. In this context, sensors are a hot topic in today's scientific community, which has developed rapidly in the past decades. Sensors are ideally highly sensitive, convenient, reproducible, flexible, and easy-to-operate analytical tools used in the food hygiene [4,5], biomedicine [6,7], microbiological detection [8,9], agricultural [10,11], and pharmaceutical fields [12,13]. In medicine, sensors use optical, electrochemical, thermometric, piezoelectric, and magnetic methods to successfully detect cells, proteins, toxins, microorganisms, and glucose, achieving satisfactory results [14,15].

Paper is a common environmental material and is flexible, cheap, environmentally friendly, and easy to obtain, perfectly matched to the current needs of sensors [16]. Meanwhile, the cellulose structure that makes up the paper can offer micropore sites for fixed analytical reagents and samples. At the same time, the capillary force can drive liquid samples to the reaction zone without any additional devices. Cellulose can also separate the whole blood or filter out unwanted large debris, allowing samples to be used with minimum pre-treatment [17]. Therefore, the application of paper-based sensors has been attractive since they were invented in the 1950s [18]. Paper-based sensors have all the advantages of paper, like ubiquity, availability, and low cost. Though analytical performances such as accuracy, sensitivity, and multithread detection still need to improve, paper-based sensors are regarded as one of the most promising types of sensors due to the continuous improvement of detection means and instruments [19–21]. Using a paper substrate with analytical techniques has enormous potential in biological fluid clinical analysis, such as for blood [22,23], urine [24,25], tears [26,27], and saliva [28,29]. Among these biofluids, the ease of collection and analysis of fluids such as saliva received more attention.

Saliva is a slightly acidic (pH = 6–7) biofluid produced in the oral cavity. The parotid, submandibular, and sublingual salivary glands secrete 90% of saliva. It consists mainly of water (94–99%), organic substances, and inorganic biomarkers [30]. These biomarkers can be used to reflect the oral cavity's physiological state. In addition, changes in the oral microbiome may contribute to localized oral diseases or systemic lesions, which can also be diagnosed by detecting microorganisms in the oral cavity. Saliva analysis is attractive because it differs from blood analysis, a non-invasive method of clinical analysis. Compared to other non-invasive tests, saliva testing can provide a larger sample size without embarrassing the patient. Saliva collection is simple and convenient, with a low risk of contamination and minimal stress to the patient [31]. Thus, sensors detecting saliva biomarkers will be promising non-invasive, simple-to-operate, cost-effective, and timely tools to satisfy personal healthcare needs. Significantly enhance the applicability of point-of-care (POC) tests, early disease diagnosis, personal health monitoring, and disease risk assessment.

There have been several reviews on saliva sensors [32–34]. However, these reviews are mainly specific to a particular assay [35] or disease [36]. Meanwhile, in the study of paper-based sensors and biosensors, no reviews focus on saliva detection [37]. Therefore, the current review summarizes the current state of biosensor research combined with saliva analysis (Figure 1). However, most of these devices have been successfully tested in the laboratory and are expected to be used commercially.

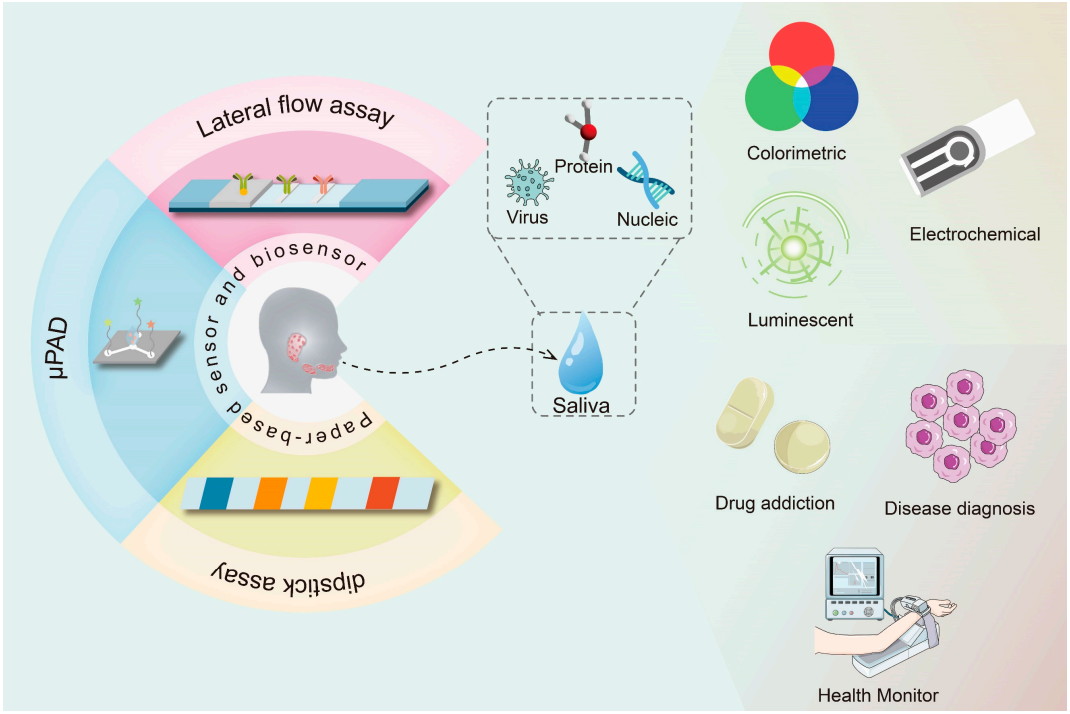

Figure 1. Overview of the paper-based sensor and applications for salivary biomarker detection.

2. Components of the Paper-Based Biosensors

As the most common material in the world, paper is unexpansive, stable, and environmentally friendly. Using the advantages of paper is one of the design directions of paper-based biosensors. Paper is used as the substrate material and can be divided into two types. The first type is represented by filter paper, which is made of cellulose and is mostly used as the substrate of microfluidic paper-based analytic devices (μPAD), while another type is called nitrocellulose membrane (NC membrane). This membrane can immobilize the protein through streptavidin-biotin interactions, so it is usually used in the lateral flow assay.

2.1. Types of Paper-Based Sensors and Biosensors

Due to the difference in materials and design methods, paper-based sensors can be classified into three types: dipstick assay, lateral flow assay, and μPAD. Each of these sensors has its characteristics and applications and is broadly used in saliva detection.

2.1.1. Dipstick Assay

Dipstick assay is similar to traditional pH test paper made from filter paper. The signal was shown directly when loading the sample into the test paper. This variation mainly manifests as a color change, so it doesn't need a particular liquid diffusion channel.

Vyas et al. reported a calixarene-based paper strip colorimetric sensor to detect copper and L-tyrosine in saliva (Figure 2a) [38]. They synthesized amide-incorporated calixarene. When Cu^{2+} in saliva was selectively detected, a color change from colorless to yellow was visible by this artificially synthesized compound. Then the Cu^{2+} complex can detect the L-tyrosine through the secondary color-to-colorless change. This molecular sensor was fabricated for use and field application to the semi-quantitative evaluation of Cu^{2+} and L-tyrosine, just like a pH test paper. Davidson et al. reported a colorimetric biosensor to detect nucleic acid sequences of pathogens in saliva (Figure 2b) [39]. They put the reverse-transcription loop-mediated isothermal amplification (RT-LAMP) strategy on paper-based devices. This biosensor has a reaction pad and a control pad, which stick to a Polyester (PET) backer. Both of them were separated using polystyrene spacers. Color changes

between red and yellow when the SARS-CoV-2 nucleic acids appear in diluted saliva. They developed a four-step colorimetric RT-LAMP dipstick assay. The sample collection step allows users to collect saliva by themselves, and the transfer step requires users to place diluted saliva onto the reaction zones of the biosensor. For the incubation step, the sample-loaded biosensor is sealed and heated at 65 °C for 60 min. Then users compare the color of the reaction and control zones. Because the pyrophosphate ions precipitated during the RT-LAMP processing, phenol red changed from red to yellow, which is visible by the naked eye and can be observed by the colorimetric reporters. Thus, the calculated specificity and sensitivity were 100% and 76%, respectively, similar to the RT-qPCR assay.

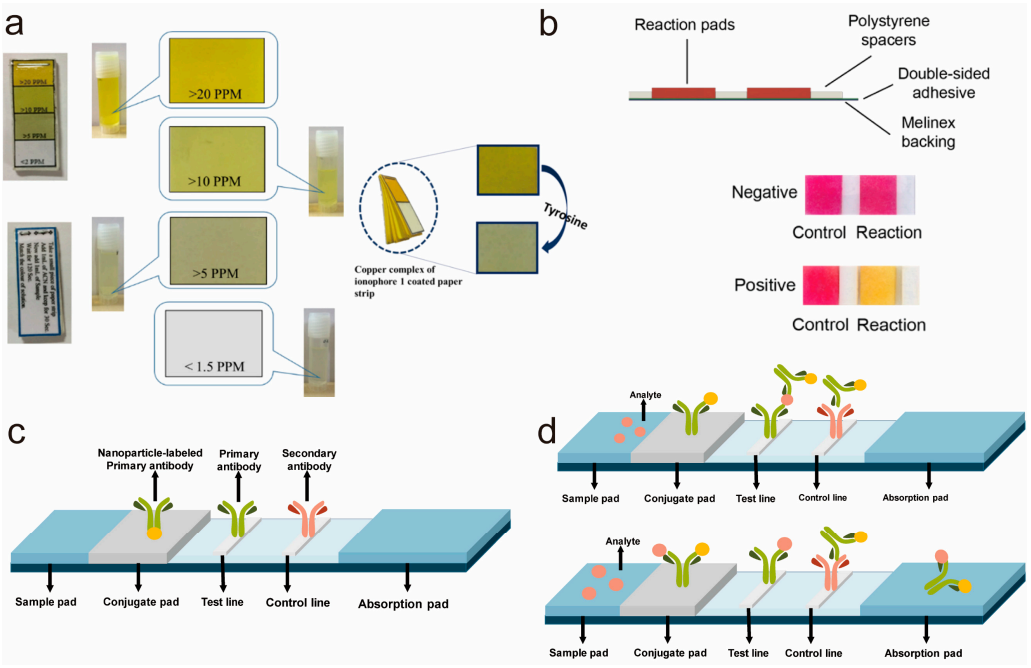

Figure 2. Different sorts of paper-based salivary sensors. (**a**) A dipstick Cu2+ and L-tyrosine salivary sensor (Reproduced with permission from Ref. [38] Copyright 2020, Elsevier); (**b**) Schematics and colorimetric characterization of the paper-based device. (Reproduced with permission from Ref. [39] Copyright 2021, Elsevier); (**c**) A standard lateral flow assay strip; (**d**) The process of sandwich lateral flow assay (**top**) and the competitive lateral flow assay (**bottom**).

It is easy to demonstrate that the dipstick assay doesn't need complicated structures and designs, and users usually need minimal steps to get visible results. Therefore, it is a user-friendly biosensor to promote point-of-care tests. However, this kind of biosensor cannot carry out accurate quantitative testing, which limits the application of this sensor.

2.1.2. Lateral Flow Assay

The lateral flow assay (LFA) is one of the most common detection methods of point-of-care tests since it emerged in the 1960s for the first time, being used for monitoring serum proteins [40]. Demand for reducing the time from specimen collection and laboratory diagnosis promotes the use of lateral flow assay, especially during the emergence of the SARS-CoV-2 pandemic [41]. As shown in Figure 2c, the standard lateral flow assay strips consist of four parts: sample pad, conjugate pad, reaction membrane, and absorption pad. When the liquid adds to the sample pad, capillary forces will drive the sample through the conjugate pad, while the target will be coupled to the receptor-conjugated tracers. The signal on the reaction membrane will show on the test line (T line) when the complex migrates to the reaction membrane. The reaction membrane is also equipped with a control line (C line) to avoid false negatives [42].

The strategies of LFA can be divided into two types: sandwich LFA and competitive LFA. In summary, sandwich LFAs are preferably implemented for analytes with large

molecules or multiple binding sites like protein. Specific nucleic acids or antibodies coat with the Test and Control lines, respectively [43]. If the sample contains targets, the signal of both lines will change, and if not, just the C line changes its signal (Figure 2d).

As we know, malaria can be transmitted by parasites. However, subclinical malaria infections are difficult to detect, leading to the massive spread of malaria by parasites [44]. To solve this situation, Tao et al. developed an LFA device to detect the female gametocyte-specific protein PSSP17, a target biomarker of the parasite in saliva (Figure 3a) [45]. Two high-affinity murine monoclonal IgG antibodies, 10E2.B7 and 27C9.B5, are attached to the strip to capture and detect the PSSP17 protein. Europium chelate (EuChelate) microparticles were conjugated onto the 27C9.B5 antibody, which can be excited by a handheld ultraviolet flashlight to emit fluorescent light. When the 27C9.B5 captured PSSP17, complexes banded to biotinylated 10E2.B7 and generated fluorescence on the T-line. This lateral flow assay strategy can identify subclinical carriage to facilitate a targeted immunization strategy that may reduce the spread of malaria. However, this current prototype strategy has not yet been verified using quantitative testing.

At the same time, many LFA tools are being developed for quantitative or half-quantitative detection. Xie et al. developed a novel magnetic/fluorescent dual-mode lateral flow immunoassay (LFIA) based on multifunctional nanobeads to rapidly determine the presence of SARS-CoV-2 nucleocapsid protein (NP; Figure 3b) [46]. They fabricated magnetic quantum dots with double QD shells (MagDQD) to generate magnetic and fluorescent signals simultaneously. The IMagDQD labels were dried on a conjugated pad and could combine with SARS-CoV-2 NP to form the immunocomplexes. Then the immunocomplexes were captured using Ab_2 on the T-line, while the goat anti-mouse IgG on the C-line captured the free IMagDQD labels. The magnetic and fluorescent signals can be measured using the immunomagnetic biosensor testing system and the fluorescent detector, respectively. This method solves the drawback that LFA can only qualitatively detect and provides a lower LOD and broader detection range than a single-signal LFA.

In contrast to sandwich LFA, competitive LFA is employed at the small molecular target or a single binding site [47]. When there are enough targets to be measured in the sample, the C-line is changed, or conversely, the T-line is altered (Figure 2d). Elizaveta et al. recently reported a lateral flow immunoassay to detect cortisol in human saliva, which is closely related to human emotional stress (Figure 3c) [48]. After the saliva and cortisol mixture was applied onto the sample pad, coloring was observed on the upper spot, indicating the antigen's concentration in the sample. After drying and scanning the test strips, the images were obtained and digitized using Image J software, and the sensitivity was 73%. Similarly, this method can detect small molecules like cotinine [49], synthetic cannabinoids [50], morphine, and methamphetamine in saliva [51].

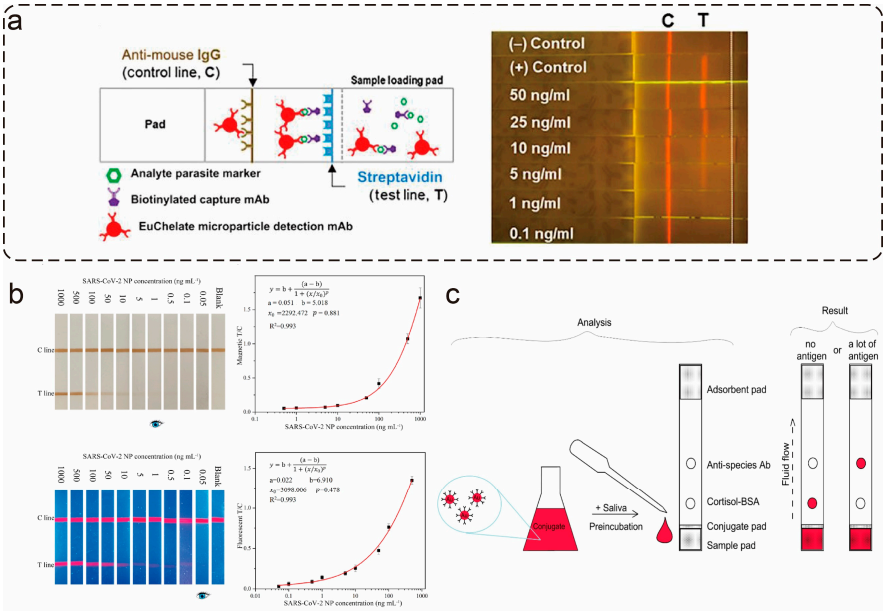

Figure 3. Sandwich and competitive salivary lateral flow assays. (**a**) Schematic of the gRAD lateral flow platform and the capture and detection of PSSP17 by EuChelate microparticle-conjugated mAbs (**left**); images of LFIA gRAD strips to estimate the LOD of recombinant PSSP17 in spiked-in assays using naïve human saliva as a matrix (**right**). (Reproduced with permission from Ref. [45] Copyright 2019, American Association for the Advancement of Science); (**b**) Photograph and fluorescent images of the dual-modal LFIA strips with different concentrations of SARS-CoV-2 NP (0.05–1000 ng mL^{-1}). (Reproduced with permission from Ref. [46] Copyright 2022, Elsevier); (**c**) The analysis procedure (**left**) and the analysis result (**right**) of cortisol lateral flow immunoassay. (Reproduced with permission from Ref. [48] Copyright 2021, MDPI). gRAD, generic rapid assay device; mAb, monoclonal antibody.

2.1.3. Microfluidic Paper-Based Analytical Device (μPAD)

In 2007, Martinez et al. reported the first microfluidic paper-based analytical device for bioassays, and μPAD has attracted much attention in biosensing due to its ease of fabrication, rapid operation, and precise interpretation [52,53]. Unlike other paper-based biosensors, classic μPADs often contain a hydrophobic barrier, a detection zone, and a microfluidic channel (Figure 4a). They are designed in different patterns on the paper so that the liquid can follow a predetermined trajectory through the substrate. The highlight of the μPAD design is the hydrophobic boundary patterning because the liquid is driven not only by the capillary forces of the hydrophilic paper but also by the hydrophobic microchannel produced by the physical barrier [54]. These barriers are commonly generated by photolithography [55], wax printing [56], stamping [57], lacquer and glue spraying [58], laser [59], inkjet printing [60], flexographic printing [61], and 3D wax printing [62]. Some unique fabrics have been used; for example, Sousa et al. reported the creation of μPAD hydrophobic barriers using a 3D pen only, without any instrumental requirements (Figure 4b) [62]. Within two simple steps, the drawing stage and the curing stage, 2 mm diameter spot tests and 3 mm width channels can be created to detect glucose and nitrite in saliva. The resulting μPAD can be obtained within 60 s and costs $0.05. This approach exhibits great potential in any setting around the world. Chauhan et al. presented a barrier-free μPAD (BF-μPAD) device to meet the needs of high-volume manufacturing (Figure 4c) [63]. BF-μPADs can detect multiple targets without the requirement of any patterning barriers. They consist of a fluid-distributing layer and a colorimetric bottom layer containing reagents. The significant difference in wicking rate ensures the liquid flow by vertical means, producing highly spatially uniform colorimetric signals and dispensing the need for hydrophobic barriers. Thus, multiplexing BF-μPADs can simultaneously detect

salivary thiocyanate, protein, glucose, and nitrite in a miniature device. One of the biggest advantages of μPADs is that they allow for quantitative testing. Francisca T.S.M. et al. reported nitrite and nitrate determination μPADs for the quantitative detection of saliva samples (Figure 4d) [64]. The nitrite μPAD consisted of an empty paper disc E1 and the reagent paper disc G1. In contrast, the μPAD for nitrate determination has an additional top layer Z, a zinc suspension paper disc. The liquid flows through the L1/E1/G1 or L1/Z/E2 layers until it reacts with the chromogenic reagent on layers G1 and G2, which produces the pink product. The bottom layer of the μPADs was then scanned and analyzed the to establish the linear relationship between the results. The intensity of the color is directly proportional to the concentration of the analyte in saliva, and a single bi-parametric device can assemble both determinations to facilitate health diagnosis.

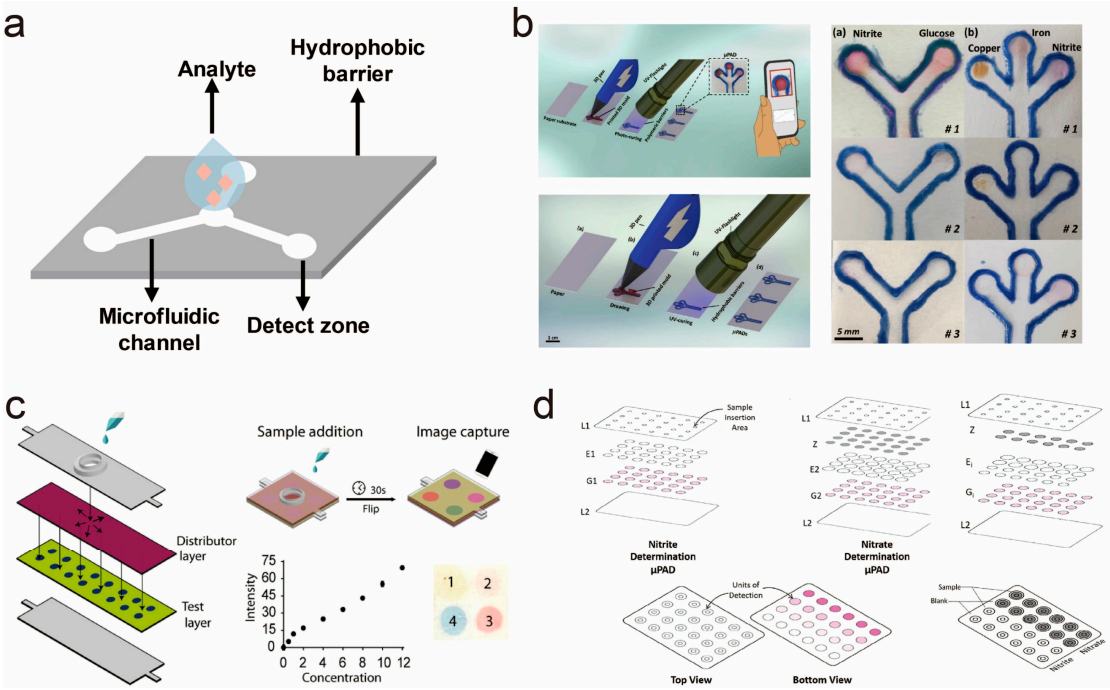

Figure 4. Microfluidic paper-based analytical device (μPAD) for salivary biomarkers detection. (**a**) A standard μPAD; (**b**) Scheme showing the fabrication of μPADs through 3D pen drawing. (Reproduced with permission from Ref. [62] Copyright 2020, Elsevier); (**c**) Design and function of the 8 cm × 2 cm BF-μPAD containing 16 detection zones (Reproduced with permission from Ref. [63] Copyright 2021, American Chemical Society); (**d**) Schematic assembly of the μPAD for the nitrite (**left**) and nitrate (**right**) determination and the schematic representation of the device after sample placement (**bottom**; reproduced with permission from Ref. [64] Copyright 2020, Elsevier). L1, **top** layer of the laminating pouch; L2, **bottom** layer of the laminating pouch; E1, empty layer; G1, Griess reagent layer; Z, zinc embedded layer; E2, empty layer; G2, Griess reagent layer.

2.2. Composite Structure

With the progressive research of paper-based biosensors, the application of biosensors is no longer limited to detecting single substances. More and more sensitive and versatile sensors have been developed for saliva-sensing applications. The paper-based sensor and biosensors gradually combined with external structures and complex strategies to meet POC requirements.

2.2.1. Sensor and Biosensors Associated with the Signal Amplification Strategy

To satisfy the detection of trace biomarkers in the sample and increase the sensitivity, sensors and biosensors were combined with signal amplification strategies, such as pre-processing samples or signal amplification components at the front of the sensor, to detect

trace biomarkers. The corresponding biomarker concentrations in saliva are lower than those in serum. Thus, the need for signal amplification strategies is more prominent than for blood sensors [65]. Laura et al. demonstrated a colorimetric smartphone-assisted biosensor for detecting SARS-CoV-2 in saliva [66]. This novel immunoassay device uses magnetic beads (MB) as a supporter to immobilize the immunological chain, a 96 well paper plate integrated with a smartphone application as a color visualization platform. MB is used as a supporter because its high surface-to-volume ratio can load large amounts of capture antibody, and the pre-concentration of MB on the biosensor using a magnetic tool can increase the sensitivity of measurement [67]. This strategy combines the magnetic beads with an immunological chain in saliva; then, the MBs are loaded onto the enzymatically modified substrate. A colorimetric signal is given after the washing steps. The detection limit is 0.1 μg/mL, demonstrating the capability to detect the Delta variant (Figure 5a). In addition to using the properties of nanoparticles for signal amplification, nucleic acid amplification technology has been extensively used to construct highly sensitive biosensors. The Rolling circle amplification (RCA) reaction is a high-sensitivity and simple signal amplification method widely applied to detecting nucleic acids as a promising tool [68].

Li et al. reported a lateral flow biosensor platform (HRCA-strip) based on the cascade nucleic acid amplification technology (HRCA) to detect salivary miRNA 31 (Figure 5b) [69]. In this study, a salivary OSCC-associated biomarker, target miRNA 31, could trigger HRCA reaction to produce G; quadruple structures conjugate with the hemin. The hemin/G-quadruplex horseradish peroxidase-mimicking DNAzyme (H/G-HRP) was enriched and catalyzed the strip to generate a significant signal. An obviously blue colorimetric signal was observed on the T-line in the presence of miRNA 31. Precisely, the miRNA 31 hybridized with complementary sequences on Strep-MBs to assemble the composite sandwich structure. Then two hairpin probes, H1 and H2, were introduced as the primers for the RCA reaction. H1 was unfolded using the initiator strand probes (Dp) and hybridized with the H2; then the opened H2 could release the sticky sequence to further unfold H1. Dp initiated a hybridization chain reaction (HCR) to generate long-strand double-stranded DNA in this way. Furthermore, the HCR circulation could trigger further RCA reactions. The HCR products hybridized with closed dumbbell padlock DNA templates to generate several G-quadruplex structures. Most HRCA products removed from MBs due to the steric hindrance effects. Then the mimic enzyme was incubated with hemin-catalyzed TMB to generate a visible blue signal on the strip. A portable, and specific miRNA 31 chromogenic detection can be achieved by this strategy.

Varona et al. adopted an alternative nucleic acid amplification strategy and achieved excellent effects (Figure 5c) [70]. Loop-mediated isothermal amplification (LAMP) is an in vitro nucleic acid amplification method that yields large quantities of DNA under constant temperature within an hour. In the previous discussion, a dipstick assay combined with LAMP has been demonstrated. Similarly, Varona reports commercially available lateral flow immunoassay (LFIA) strips using molecular beacon (MB) probes for the specific detection of LAMP sequence. The ompW gene from Vibrio cholera, BRAF V600E SNP, and ORF1a gene of SARS-CoV-2 have been detected successfully. Briefly, MBs are stem-loop structure double-labeled oligonucleotide probes. One of the loop primers is combined with fluorophore-labeled MB, while the other is biotinylated. The LFIA strip imparts specificity by the MB, biotinylated primer and the amplicon hybridized. This detection scheme adopts real-time fluorescence detection and yields identical sensitivity.

In 2018, the invention of the CRISPR/Cas-based biosensor represented by SHERLOCK and DETECTOR contributed to the widespread use of CRISPR as a powerful instrument in biosensors [71,72]. CRISPR/Cas is mainly used in nucleic acid sequence detection for further signal amplification and output, and the Cas protein specifically recognizes signal amplification products to activate cleavage activity, then acts on the designed substrate to achieve the signal amplification effect [73]. In the field of paper-based saliva sensors, Park et al. applied reverse transcription recombinase polymerase amplification (RT-RPA) and reverse transcription loop-mediated isothermal amplification (RT-LAMP)to construct a lateral

flow assay for specifically detecting influenza A (IAV) and B (IBV) viruses (Figure 5d) [74]. After influenza virus RNAs were amplified using RT-RPA and RT-LAMP, the detector detected amplicons in the lateral flow assay. After the signal amplification mixture was applied on a strip, the result was inferred within 2 min, which can sensitively and specifically detect IAV and IBV.

Chen et al. have also designed the cascade signal amplification scheme of "invading stacking primer" (IS-primer) amplification reaction (ISAR). Dual-mode paper-based strip (dm-Strip) coupling with CRISPR/Cas12a and ISAR detect hsa-miRNA 31-5p (miR-31; Figure 5e) [75]. ISAR was activated by the miR-31, which would further trigger the Cas12a protein to cleavage the nonspecific single-stranded DNA (ssDNA). SsDNA was labeled with digoxin and biotin on the termini, which could generate the fluorescent signal and colorimetric visual signal on the designed dm-Strip. The ISAR/Cas12a-dmStrip biosensor could realize an ultrasensitive and portable detection to improve the patient's postoperative life quality.

2.2.2. Sensor and Biosensors Combined with Intelligence

In addition to analytical capabilities, the sensor and biosensor paradigm is shifting in a more intelligent direction. Sensors and biosensors combined with smart devices can quantify biomarkers more accurately and reduce detection limits. It can also facilitate medical development in resource-limited areas by uploading signals to the medical Internet of Things (MIoT) in real-time with the help of powerful cloud-based medicine. The biggest issue while using smart devices for signal detection is the difference in reading between devices. Some strategies are dedicated to solving this problem. Based on a colorimetric reaction, Fan et al. designed a smartphone-assisted microfluidic paper-based analytical device (SμPAD) quantification of salivary uric acid (UA; Figure 6a) [76]. The UA detection can be quantized by Prussian blue sediment, which is generated by the potassium ferrocyanide in the presence of UA. Then, potassium ferrocyanide produces a blue precipitate after it reacts with ferric chloride. To quantify the intensity of the color signal, a smartphone APP coded by MATLAB was developed; it can automatically recognize the test zone and the standard color bar on SμPAD, then take the measurement color calibration. After color correction, signal deviation due to external ambient light was eliminated. Therefore, using this procedure, the distinction between signal readout or photographs taken by the different cameras can be effectively eliminated, providing a trustworthy result. Intelligent devices that integrate machine learning or deep learning can also enhance detection accuracy and facilitate self-health monitoring by users.

Mercan et al. developed a portable μPAD platform incorporating an application on a smartphone to quantify glucose concentration in artificial saliva (Figure 6b) [77]. The images of the μPADs were analyzed with four different devices under different backgrounds after the signal change. The image analysis was based on machine learning classifiers. After extracting the images feature and machine learning classifiers training, a robust optics platform was built. A user-friendly application called "GlucoSensing" can capture images based on the best machine learning classifier. Machine learning classifiers were also interfaced with the cloud system to provide the highest classification accuracy (98.24%) in detective TMB mixture under ambient light without any restriction. The proposed method has a massive prospect in the non-laboratory to detect glucose.

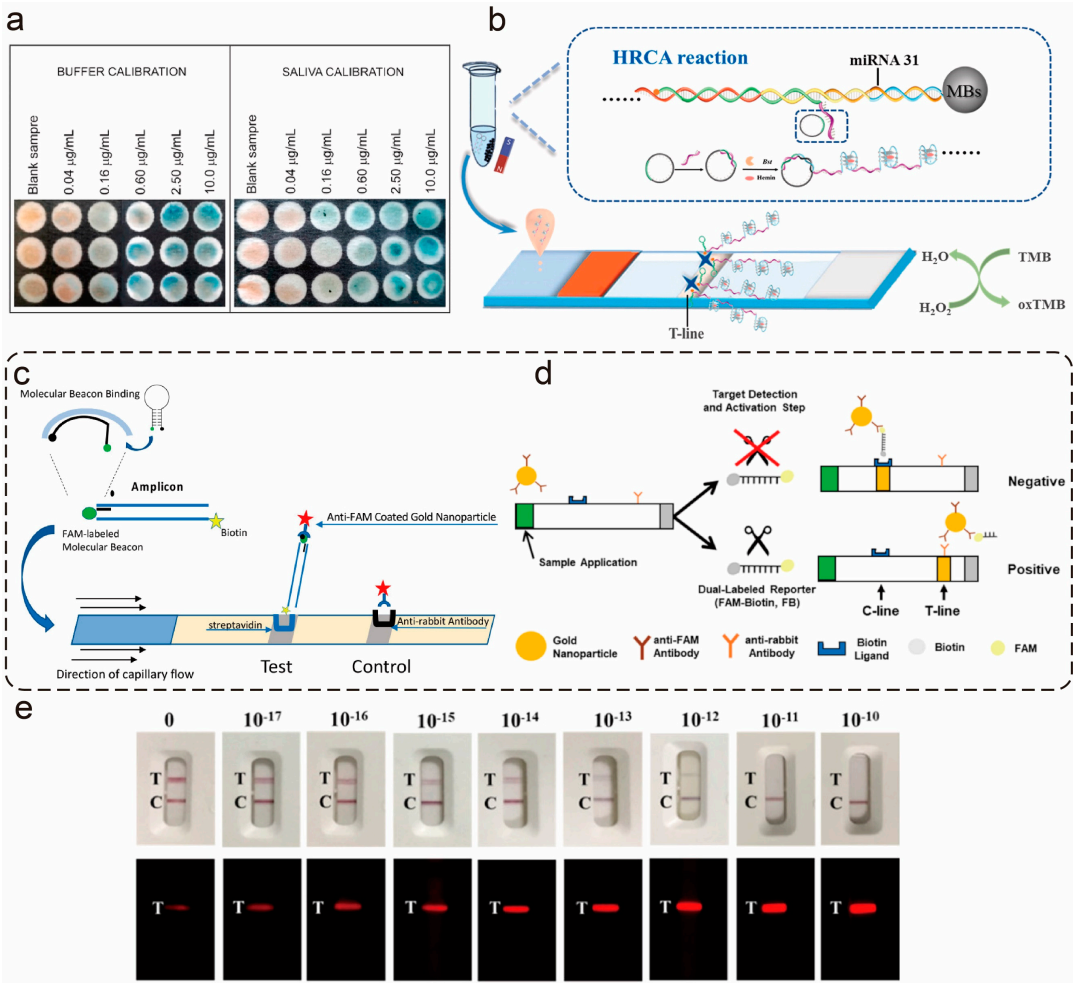

Figure 5. Salivary sensors associated with the signal amplification strategy. (**a**) Calibration images for Spike protein detection in buffer and untreated saliva (reproduced with permission from Ref. [66] Copyright 2022, Elsevier); (**b**) Schematic illustration of the HRCA-strip for miRNA detection based on HRCA reaction (reproduced with permission from Ref. [69] Copyright 2022, Elsevier); (**c**) Schematic representation of MB-LAMP detection on a commercially available LFIA strip (reproduced with permission from Ref. [70] Copyright 2021, American Chemical Society); (**d**) Schematic diagram showing how to distinguish between positive and negative results in a lateral flow strip (reproduced with permission from Ref. [74] Copyright 2021, MDPI); (**e**) Visual and fluorescent photographs for various concentrations of microRNA-31 (reproduced with permission from Ref. [75] Copyright 2020, Elsevier). MB, magnetic beads; FB, FAM-Biotin.

2.2.3. Multiplex and Multi-Dimensional μPAD

Under the requirement of multi-analyte or multi-function detection with minimal sample requirements and the development of paper-based sensors, multiplexed and 3D-μPAD sensors have been gradually applied for their absolute advantages in analysis throughput over single assays [78]. Compared with single-biomarker detection, multiplexed sensors provide the simultaneous detection of a panel of discriminative biomarkers, which can efficiently improve the accuracy of detection [79]. A classical multiplexed saliva biosensor reported by Pomili et al. included three microfluidic channels for the multiplexed detection of glucose, cholesterol, and lactate (Figure 6c) [80]. When the saliva is dropped onto the sample zone, it can drive through the microfluidic channels and is then mixed with NaI in the pretreatment zones before entering the sensor zone. NaI, as a halogen, boosts the oxidation process and could promote a rapid color change. The color change relies on multibranched GNPs (MGNPs) in the sensor zone. MGNPs are visible blue and fixed

with oxidase enzymes (cholesterol oxidase (ChOx), glucose oxidase (GOx), and lactate oxidase (LOx)), respectively. When the biomarker mixes with the oxidase enzyme, the byproduct (H_2O_2) is converted into its free radical form and etches the MGNPs, promoting a color shift from blue to pink. The reaction occurs within a few minutes with a visual qualitative readout taken using the naked eye and a smartphone camera. During multiplex sensing, the sample flow inevitably had an unwanted diffusion which contaminated the undesired molecules. To avoid cross-contamination and maintain the high specificity per channel, Yu et al. developed a specific paper-based five petal microfluidic platform [81]. The hydrophilic channels arranged into five petal shapes on paper transport the sample to the sensing channels. Five pairs of extra wax barriers were employed to avoid cross-contamination (Figure 6d). Meanwhile, they used paper bridges to guarantee the transportation of liquids. For the saliva detection, the sensitivities (slopes) to human serum albumin (HSA) and human immunoglobulin G (HIgG) were 100.12% and 88.67% to those in phosphate buffer, respectively.

Compared to 2D µPAD, 3D µPAD has the advantage of a rapid liquid flow in the vertical direction and the simultaneous performance of multiple experiments [82]. In particular, saliva is more viscous than other biofluids, and reducing the negative effect of viscosity is more needed. Origami-based 3D paper microfluidic devices (oPADs) is one kind of 3D µPADs, and the reaction can be induced through a simple manufacturing and folding process [83]. To standardize the fabrication and reduce assembly errors, Yu et al. demonstrated an origami wax-patterned device based on a multiplex microfluidic platform that uses the same idea as the previous research, as shown in Figure 6e, the origami biosensor includes a sample-splitting layer, a multiplexed detect layer, and an absorbing pad in the bottom. The sensing ability of the origami biosensor was comparable to the previous layer-by-layer assembled one, but the production process is much more industrialization. Bordbar et al. propose an origami E-tongue to diagnose SARS-CoV-2 by analyzing the metabolites of saliva samples (Figure 6f) [84]. Each column of the E-tongue delegate unique classes of the receptor. When exposing the saliva sample biomarkers to the origami-based sensor, the color changes and composition show special electronic fingerprint patterns after 4 min. Patient, healthy, and cured samples show their unique fingerprint colorimetric patterns on the sensor. This could be used to predict the severity of symptoms by assessing the viral load.

Undoubtedly, the design of intrinsic structures or integration with external systems is important for developing paper-based sensors. Although many advantages of composite paper-based biosensors have been mentioned above for practical diagnosis and POC applications, many significant challenges remain to be overcome. The major drawback of the multiplexing sensor is that the number of multiplexed assays increases the risk of observing interference in detecting different analytes. Furthermore, fabricated sensor production increases the complexity of development and usage. Cross-contamination between different detection channels should also be considered. Thus, the user-friendly interpretation methods, the industrial production-ready sensor structure, and the integration with the intelligent device are expected to dominate the biosensor development field in the foreseeable future.

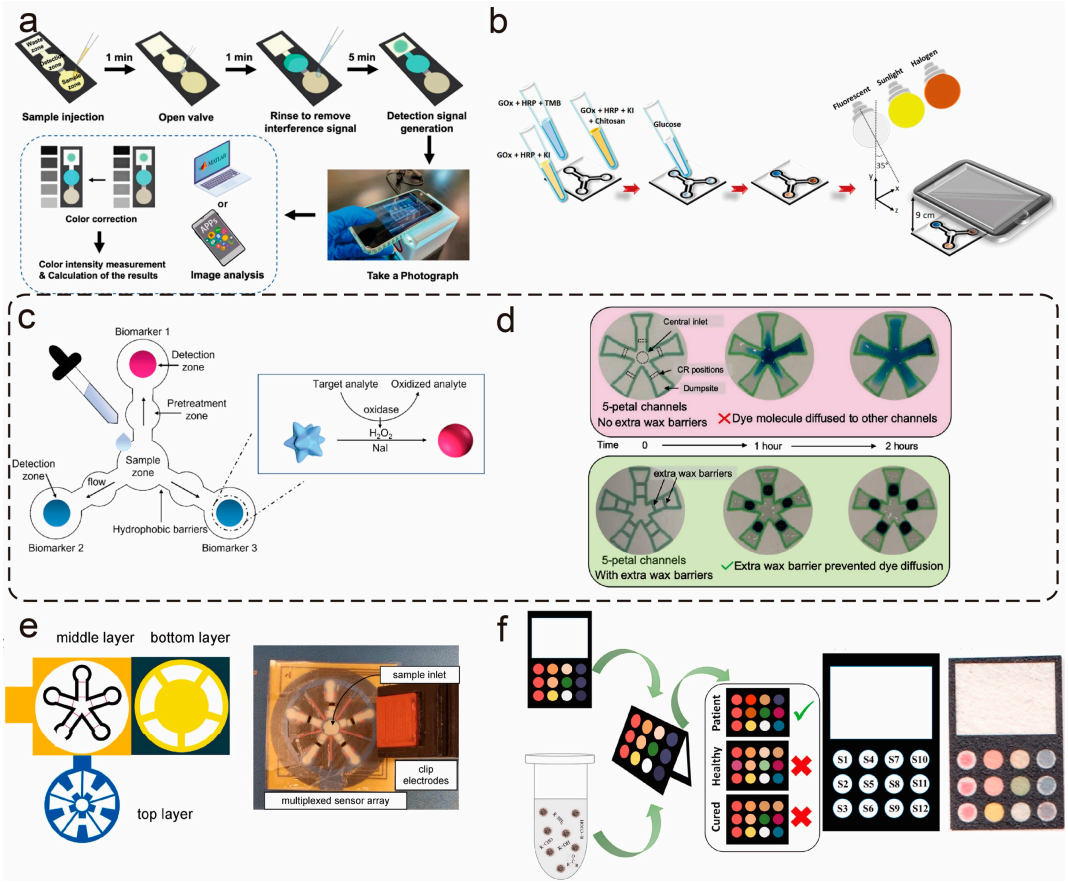

Figure 6. Sensors combined with intelligence or multiplex and multi-dimensional construction. (**a**) Smartphone-Assisted μPAD (SμPAD) for the Colorimetric Detection of UA (Reproduced with permission from Ref. [76] Copyright 2022, American Chemical Society); (**b**) Schematic illustration of the glucose determination strategy. The change in color in the detection zones of the μPAD was imaged using a smartphone camera under various combinations of fluorescent, halogen, and sunlight sources. (Reproduced with permission from Ref. [77] Copyright 2021, Elsevier); (**c**) Schematic illustration of the monolithic paper-based device for the simultaneous detection of three salivary biomarkers. (Reproduced with permission from Ref. [80] Copyright 2021, MDPI); (**d**) Design of the five petal microfluidic channels with (**top**) and without (**bottom**) extra wax barriers. (Reproduced with permission from Ref. [81] Copyright 2021, Elsevier); (**e**) Sensing protocol and image of the origami device. Assembly of the three-layered origami device (**left**); image of the origami device with clip electrodes attached (**right**). (Reproduced with permission from Ref. [84] Copyright 2021, Elsevier); (**f**) The schematic diagram for the design of a salivary E-tongue and the image of the proposed sensor array. (Reproduced with permission from Ref. [84] Copyright 2022, Elsevier). UA, Uric acid.

3. Detection Methods

Due to the different detection methods and signal changes, sensors based on various sensing methods have been developed. Each of these methods has its pros and cons. This section focuses on the variety of paper-based saliva sensor detection methods and their advantages and disadvantages.

3.1. Colorimetric

Colorimetric sensors transform detection events into color changes [85]. Colorimetric analysis is one of the most common paper-based microfluidic sensing and directly visible detection methods. Color change can come from the transformation of nanoparticles or the redox reaction of the chromogenic substance. Among them, the gold nanoparticles (AuNPs)

provide excellent platforms for colorimetric sensors as they can be easily changed by localized surface plasmon resonance effect (LSPR)and functionalized with protein or nucleic acid [86,87]. Oh et al. synthesized new plasmon color-preserved AuNP clusters to detect SARS-CoV-2 nucleocapsid proteins using the lateral flow assay platform (Figure 7a) [88]. The AuNP clusters improve the sensitivity compared with the isolated individual AuNPs, but the original color is maintained. To avoid plasmon coupling lowering the absorption in the visible range between AuNPs, AuNPs coated with biotinylated antibody-streptavidin are linked to form a nanoscale gap, thus maintaining the red color while increasing the light absorption. The limit of detection (LOD) of the AuNP clusters is dozens of times lower than the standard lateral flow assay for detecting SARS-CoV-2 nucleocapsid proteins.

Prainito et al. reported a salivary SARS-CoV-2 spike protein biosensor made using paper-based polydiacetylene (Figure 7b) [89]. They took advantage of a color change when exposing Polydiacetylenes (PDAs) to targeted proteins. The PDAs were coated on a polyvinylidene fluoride (PVDF) paper strip. When the spike protein antibody interacted with the immobilized antibody incubated in PDAs, the biosensor displayed a noticeable color change from blue to red upon exposure to UV light. Users can scan the sensing pad and upload data using a smartphone app.

In summary, the colorimetric method is simple in its design and intuitive in its results. The straightforward signal output allows the user to avoid complicated training. Therefore, it is suited for combination with paper-based sensors and be applied in the POC field. However, this detection method could cause controversial readouts due to the visual bias of the operators, especially when the detection signal is close to the threshold. At the same time, the difficulty of quantification means that this method only works as a rough detection tool. Therefore, there have been some colorimetric paper-based sensors combined with intelligent devices to improve the above disadvantages. In contrast to Prainito et al.'s work, Kim et al. reported a colorimetric smartphone-based alcohol sensor combined with optical attachment and machine-learning algorithms to obtain a uniform alcohol strip picture (Figure 7c) [90]. An application called SPAQ2 was developed based on four color spaces matching three machine-learning algorithms. Smartphones and servers simultaneously provide alcohol concentration analysis to eliminate the impact of equipment and environment on results.

3.2. Electrochemical

One of the limitations of conventional paper-based sensors is the need for more sensitivity, especially of saliva samples and their inherently lower analyte concentrations [91]. Paper-based electrochemical sensors combine sensitive electroanalytical methods with the inherent bioselectivity of the biological component, exhibiting several unique advantages to compensate for this disadvantage. A disposable electrode μPAD eliminates the complicated cleaning steps compared with common electrodes and reduces the requirement for laboratory [92,93]. Electrochemical-based sensors can be divided into conductometric, voltammetric, amperometric or coulometric and potentiometric, depending on the different measurable parameters [94,95]. Different electrochemical techniques like cyclic voltammetry (CV), differential pulse voltammetry (DPV), square-wave voltammetry (SWV), and electrochemical impedance spectroscopy(EIS), and potentiometry represent the most used electrochemical techniques for detection in paper-based biosensor [96]. Choosing an appropriate electrochemical method is critical for designing a good performance sensor.

Sensors based on differential pulse voltammetry (DPV) have been intensely used for their higher sensitivity than amperometric sensors. Huang et al. demonstrated a salivary uric acid (UA) analysis device for the paper-based DPV technique (Figure 7d) [97]. Poly (3,4-ethylene dioxythiophene; PEDOT-GO) nanocomposite was cumulative on the indium tin oxide (ITO) substrate. The PEDOT-GO has an excellent electrocatalytic oxidation ability of UA. The sensor is sensitive to UA because the peaks of DPV detected increased linearly with the UA concentration. Good reliability is provided in detecting artificial saliva and authentic saliva samples. Jutamas et al. also used differential pulse voltammetry tech-

nology to quantify the receptor binding domain (RBD) spike protein of SARS-CoV-2 on a paper-based biosensor (Figure 7e) [98]. The screen-printing method fabricated the detection part while immobilizing the mAb CR3022 onto the surface of the working electrode. After the addition of the target RBD, the current change via $[Fe(CN)_6]^{3-/4-}$ is measured. As the RBD concentrations increased, it was shown that the signal of $[Fe(CN)_6]^{3-/4-}$ decreased. This device can be easily converted to other electrochemical sensors by switching the capture probe, which broadens the sensor's range of applications. Electrochemical techniques can also be combined with lateral flow devices (LFD). Loric et al. demonstrated an electrochemical lateral flow device for quantitatively detecting salivary C-reactive protein (Figure 7f) [99]. The sample pad contained ascorbic acid monophosphate (AAP), and the conjugate pad contained an enzymatically labeled probe antibody. The enzyme, enriched on the test line when the antibodies capture C-reactive protein, converts the AAP into the ascorbic acid (AA), and the generation of electroactive substances is locally enhanced. The specific current of C-reactive protein can be measured by applying an oxidizing voltage onto the T-line working electrode, turning AA into dehydroascorbic acid (dAA). This study has multiplexing potential in electrochemical lateral flow devices.

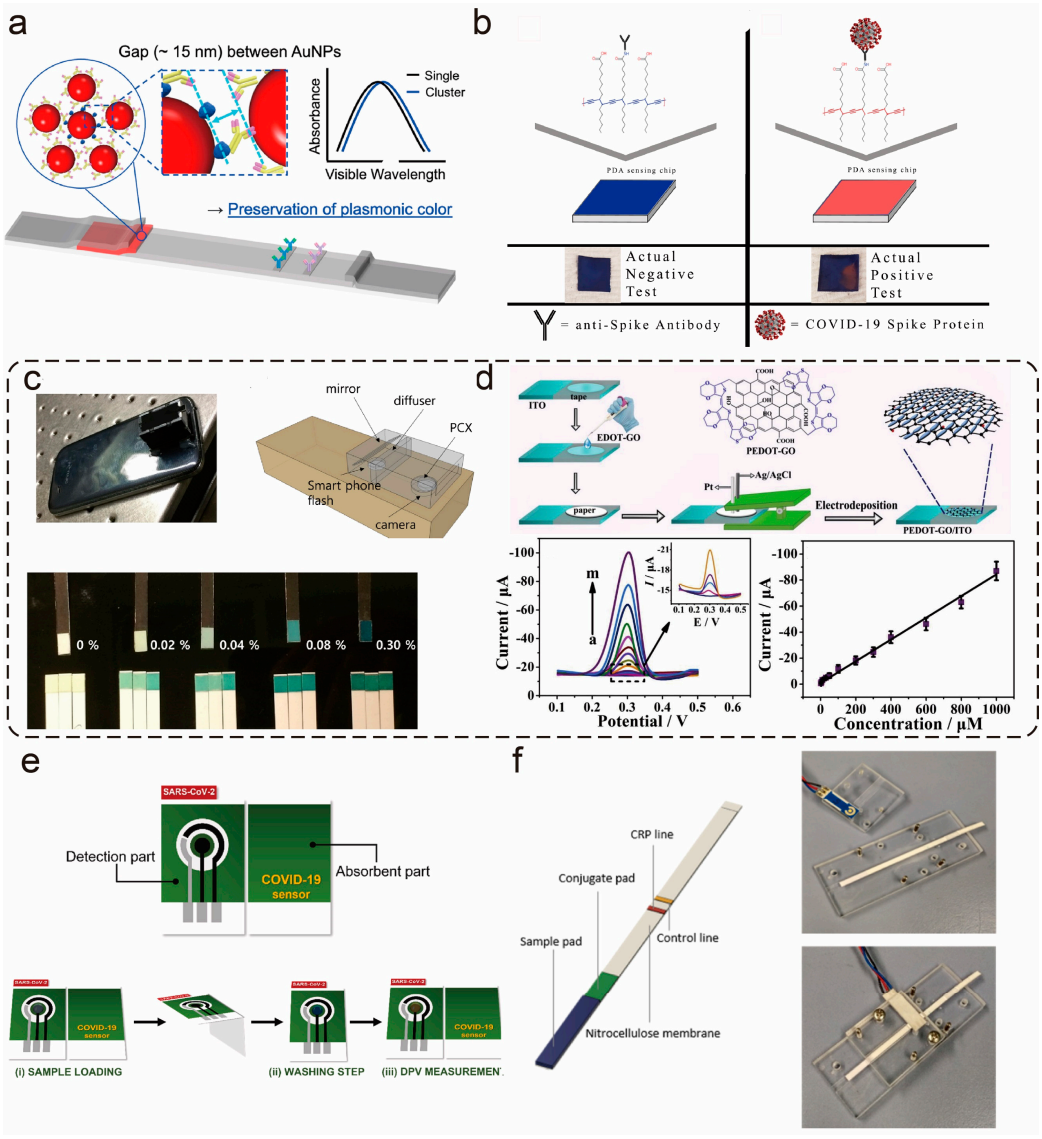

Figure 7. Colorimetric and electrochemical salivary sensor. (**a**) Schematic illustration of PLASCOP AuNP clusters incorporated within an LFI for the detection of SARS-CoV-2 (Reproduced with permission

from Ref. [88] Copyright 2022, Elsevier); (**b**) Creation of polydiacetylen-based sensor, PVDF membranes were dipped into the prepared chloroform solutions. (Reproduced with permission from Ref. [89] Copyright 2022, MDPI); (**c**) Photograph of a smartphone with a colorimetric imager attachment and schematics of the optical attachment to capture the colorimetric images (**top**); color comparison between the printed reference color chart and color changes for five different reference concentrations (**bottom**). (Reproduced with permission from Ref. [90] Copyright 2017, Optica Publishing Group); (**d**) Preparation of the integrated paper-based analytical devices (**top**); Different concentrations of UA recorded with the sensor in artificial saliva and the linear relationship between the peak current and the UA concentration. (Reproduced with permission from Ref. [97] Copyright 2020, Elsevier); (**e**) The design of paper-based electrochemical immunosensor. (Reproduced with permission from Ref. [98] Copyright 2023, Elsevier); (**f**) Schematic and pictures illustration of the electrochemical lateral flow device. (Reproduced with permission from Ref. [99] Copyright 2022, Elsevier). PLASCOP, plasmon color-preserved; PEDOT, Poly (3,4-ethylene dioxythiophene); GO, Graphene oxide; ITO, indium tin oxide; EDOT, 3,4-ethylenedioxythiophene.

Electrochemical methods can be connected with intelligent devices for readily available electronic read-out, which points the direction for miniaturization and integration. Moreover, electrochemical detection methods are not dependent on external conditions like illumination. Though the results of electrochemical sensors are not intuitive enough currently, while the operator requires professional training, these disadvantages do not affect the electrochemical sensors in situ application of the great potential with the miniaturization of the electrochemical workstation.

3.3. Luminescent

Luminescent analysis has gained massive interest due to its high sensitivity, easy operation, significant signal changes, popularized equipment, and superb spatiotemporal resolution [100]. Chemical luminescence (CL) is a luminescence phenomenon in which photons are emitted through a chemical-induced reaction yielding a product in its singlet electronically excited state. According to the different luminous mechanisms, Chemical luminescence-based sensors, including chemiluminescence sensors, bioluminescence (BL) sensors, electrogenerated chemiluminescence (ECL) sensors, and thermochemiluminescence (TCL) sensors [101]. The high signal-to-noise ratios can be obtained because the light is produced chemically. Moreover, different from photoluminescence, measuring CL strength only requires miniaturization instrumentation, no external light sources or filters. Roda et al. reported a thermochemiluminescent Vertical flow immunoassay (VFIA) biosensor which applied a one-step competitive immunoassay to detect valproic acid (VPA) ion (Figure 8a) [102]. A smartphone coupled with a TCL-VFIA system powered the mini-heater to trigger the TCL reaction, then take the image signals of the sample by the camera. TCL is one of the chemical luminescence reactions triggered by heat, no reagents need to be added. The LOD of VPA is 0.05 μg mL^{-1} in saliva.

Bioluminescent offer simple assay analysis using enzyme-catalyzed oxidation reactions to generate excited-state emitters and does not require light stimulation either. The signal is visible to the naked eye in the dark situation [103]. Bioluminescence assays can also provide a 10–1000-fold lower detection limit than fluorescent assays, providing higher sensitivity. Hunt et al. proposed a bacteria-based cell-free protein synthesis (CFPS) diagnostic platform for detecting viral pathogens by inexpensively bioluminescence technology in saliva (Figure 8c) [104]. A portable, cheap LDPE test cassette housing five separate paper-based CFPS reactions was developed to facilitate actual deployment in POCT. The CFPS system can detect control groups, replicate tests, or detect multiple pathogen nucleic acids in a similar process, showing viability for weeks. Using the NanoLuc luciferase (NanoLuc) as a bioluminescent reporter, which is responsive to the substrate furimazine. The SARS-CoV-2 RNA sequences successfully produce bioluminescence in paper-based CFPS biosensors, which is visible in a dark room. Functional activity can maintain for seven weeks.

Rare-earth doped upconversion nanoparticles (UCNPs) are powerful luminescent reporters which are excited in the infrared region and emission in the visible domain. These nanophosphors materials show high photostability, large Stokes shifts, and high quantum yields. Variations of lanthanide dopants and the host matrix can regulate optical properties. The UCNP sensor is a photoluminescence sensor with a very high signal-to-noise ratio because the interfering biomolecules absorb in the UV region while the UCNP excites with IR radiation [105,106]. Using UCNP particles as the reporter, the Up-converting phosphor technology-based lateral flow assay (UPT-LFA) displayed accurate quantitative capability and higher sensitivity compared with the traditional LFA. Hu et al. established an up-converting phosphor technology-based lateral flow assay (UPT-LFA), called Mop-UPT-LFA, and Met-UPT-LFA detecting morphine and methamphetamine as a point-of-collection testing (POCT) method (Figure 8b) [51]. To prepare UCP-antibody conjugates, UCNPs were covalently conjugated to the anti-morphine and anti-methamphetamine McAb, or goat IgG. In a positive result, morphine (or methamphetamine) blocked UCNP-McAb, and only UCP-[goat IgG]- [rabbit anti-goat IgG] formed on the reaction membrane. Based on a competitive method, this device could quantitatively detect 5–100 ng mL^{-1} and 10–250 ng mL^{-1} of morphine and methamphetamine, respectively, with a coefficient of variation <15%.

The luminescent biosensor is attractive of its simplicity, high sensitivity, and good reproducibility. However, they need to be functionalized and designed carefully to conjugate and identify the target analyte [107]. Furthermore, the results are susceptible to interference from ambient light variations. However, the luminescent sensor is still a very promising diagnostic method.

3.4. Multi-Mode Sensor

Monitoring biomolecular is an essential requirement for studying complex biological processes and diagnosis of disease [108]. Consolidating multiple measurements means in one sensor can overcome the disadvantages associated with a standalone. Therefore, multi-mode sensing strategies emerged. These strategies compensate for the shortcomings of each technique and facilitates cross-validating between results. Colorimetric and electrochemical analyses are two of the most integrated means applied to μPADs because of their portability and simplicity. Roda et al. demonstrated gold nanoparticles and horseradish peroxidase modified optical/chemiluminescence LFIA to detect the IgA specific to SARS-CoV-2 in saliva (Figure 8e) [109]. Precisely, nanogold-labeled anti-human IgA generated the color signal, which can be measured using a smartphone camera. A portable device based on cooled CCD offers a light signal for the chemiluminescence transduction produced by HRP-labelled anti-human IgA's interaction with the substrate. This IgA-LFIA approach reveals salivary IgA with excellent consistency between both detection methods. Similarly, Jyoti et al. reported a dual (electrochemical and colorimetric) vertical flow assay immunosensor for detecting influenza viruses (Figure 8d) [110]. Dual-mode sensor method provides double assurance. The VFA sensor was fabricated by stacking basic lateral flow assay components. As the virus concentration increased, the color intensity decreased on the colorimetric zone because less HRP-Ab free of H1N1 was captured. While the H1N1-HRP-Ab concentration increased, the semi-circle diameter in the Nyquist plots decreased, which is consistent with the DPV measurements.

Moreover, the dual-mode sensor approach can broaden the dynamic range of the biomarker. Kingkan et al. introduced another dual-mode sensor to solve this situation (Figure 8f) [111]. They construct a hollow capillary channel as a micropump on paper devices to facilitate viscous fluidic transport. Briefly, μpumpPAD consists of two components: the colorimetric PAD (cPAD) and the electrochemical PAD (ePAD) for colorimetric and electrochemical detection, respectively. By putting the cPAD onto the ePAD, the device assembly was completed. The higher level of SCN^- is detected by the color change, while the lower limit can be caught via an electrochemical mode by copper (II) phthalocyanine-modified screen-printed graphene electrode (CuPc/SPGE). To operate the μpumpPAD, put saliva on the sample inlet zone, and the sample will rapidly reach the colorimetric detection

zone. Herein, the Fe^{3+} on the detection zone conjugate with the SCN^- and outputs a visualized $[FeSCN]^{2+}$ complex for colorimetric detection. Square wave voltammetry (SWV) can be performed for electrochemical assay. Slid the ePAD upward to ensure the sample zone of the cPAD is in contact with the ePAD. Then, cut along the devices' dashed line to eliminate the sample's convective fluid flow. The whole device can be taken as a vertical flow assay. Then, flushing the cPAD with an electrolyte solution to ensure the remaining saliva down to the ePAD, the SWV experiment could perform. Under the two sensing modes, an extensive SCN^- dynamic range was obtained between 0.025 and 100 mmol L^{-1}. Benefiting from the above advantages, combining multiple sensing methods can increase the amount of sensor information and detection accuracy, demonstrating its enormous potential for development.

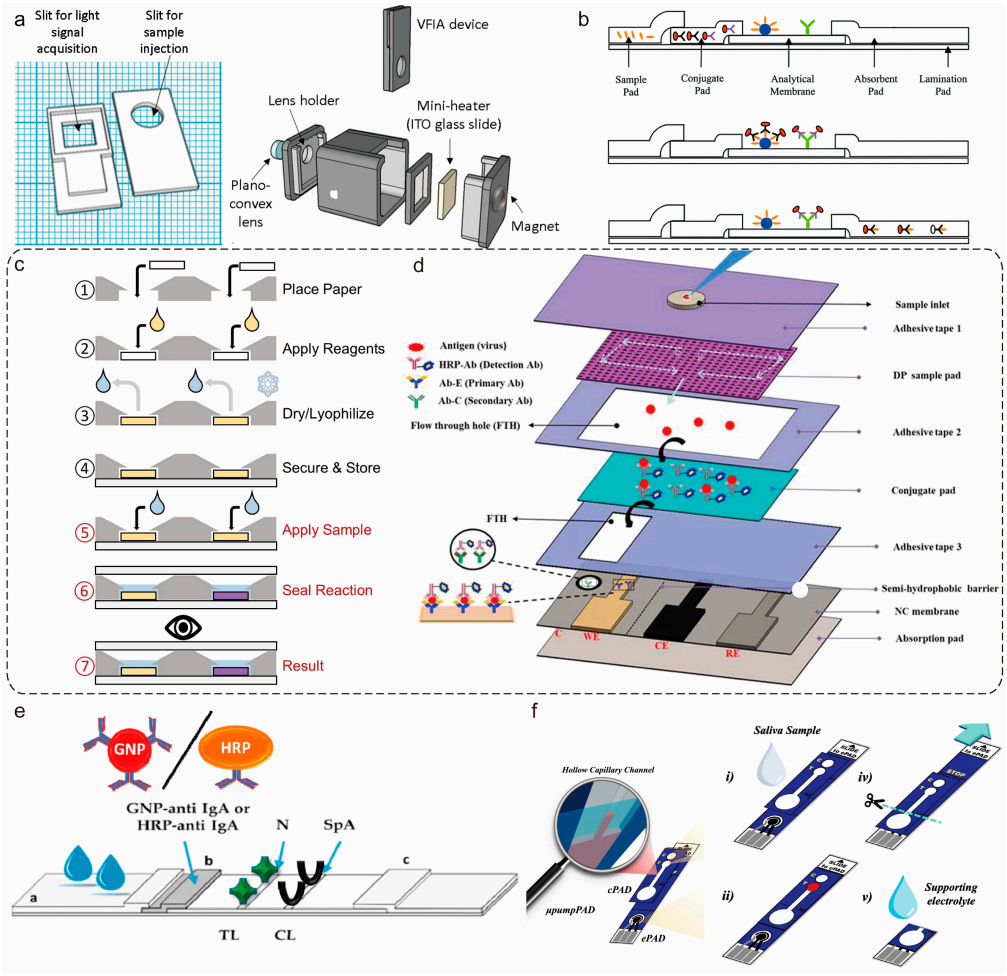

Figure 8. Luminescent and multi-mode sensor salivary sensor. (**a**) 3D model of VFIA cartridge (**left**); Scheme of the integrated TCL-VFIA device (**right**). (Reproduced with permission from Ref. [102] Copyright 2019, Elsevier); (**b**) Schematic of Mop-UPT-LFA (or Met-UPT-LFA) strips. (Reproduced with permission from Ref. [51] Copyright 2018, Royal Society of Chemistry); (**c**) The Schematic of the paper-based CFPS diagnostic test. (Reproduced with permission from Ref. [104] Copyright 2022, Elsevier); (**d**) Schematic of the integrated vertical flow assay device for dual detection (Reproduced with permission from Ref. [110] Copyright 2019, Elsevier); (**e**) Scheme of the LFIA strip used for the optical immunosensor (a: sample pad; b: conjugate pad; c absorption pad). (Reproduced with permission from Ref. [109] Copyright 2021, Elsevier); (**f**) Schematic illustration of the hollow capillary channel and the assay procedure of the μpumpPAD for dual-mode sensing via colorimetric detection on cPAD and electrochemical detection on ePAD (**i**–**v**). (Reproduced with permission from Ref. [111] Copyright 2021, Springer Nature). VFIA, vertical flow immunoassay.

4. Potential Applications

Paper-based sensors can detect multiple biomarkers with various methods associated with promising application scenarios. In the medical field, sensors can be utilized for judgment in the areas of disease prevention, diagnosis, prediction, and prognosis. At the same time, it can also be used for drug detection with a few microliters of saliva.

4.1. Disease Diagnosis

Cancer remains a major life-threatening health disease known as one of the leading causes of death. Early detection is considered the most effective, inexpensive therapy to reduce the patient's pain [112]. Telehealth can significantly increase access to cancer treatment and improve cancer prevention and control [113]. Furthermore, funding cancer prevention and treatment is far cheaper than funding treatment for the disease. Therefore, it is important to develop a more affordable, simple sensor to cater to the need for POC and prevention. The paper-based sensor has natural material advantages for making this type of sensor. Zhou et al. presented portable exosomal miRNA Lateral flow immunoassays (LFAs) to diagnose lung cancer (Figure 9a) [114]. The biosensor includes three parts: Fe3O4@SiO2-aptamer nanoparticles (FSAs) to concentrate the exosomes, duplex-specific nuclease (DSN) to achieve hydrolysis of reporter DNA triggered by exosomal miRNA, and lateral transverse flow test strips for readout. This lung cancer diagnosis kit (LCDK) uses clinical salivary and urine successfully distinguish lung cancer exosomes from the normal cell, achieving high sensitivity and selectivity of lung cancer.

A global health crisis in the making by the SARS-CoV-2 since 2019, the isolation of patients from the healthy population is the most effective strategy to prevent the rapid spread of the disease [115]. Thanks to the wild use of commercialized COVID-19 lateral flow assay, which reduces a lot of pressure on hospitals to test for the virus. From now on, many sensors have been developed to mitigate the crisis, which can effectively detect the biomarkers of COVID-19 by saliva. Patarajarin et al. reported the use of a paper-based microfluidic chip (Figure 9b) [116]. The user was required to ensure the sample was put onto the sensor and dried, then conjugate the SARS-CoV-2 nucleocapsid and submicron polystyrene particle, which was loaded the suspensions onto the sensor and flowed for 2 min. The whole process recorded the video above the chip by smartphone. A Python code for image processing was developed to analyze the result. This unique chip can determine infection status by analyzing the flow profile, which is not affected by variations in the background.

The saliva-detected paper-based sensor can detect many other diseases like the Influenza H_1N_1 virus [117], inflammatory arthritis, gout [76], and periodontal diseases [118].

4.2. Health Monitor

Continuous health monitoring is preferable to traditional healthcare workflows. Saliva is a non-invasive diagnostic method capable of painless daily physical health monitoring and maintaining the life and health of patients. Cortisol is a steroid hormone that is associated with psychological stress. Cortisol levels are important in maintaining health and need to be monitored consistently. Therefore, Hyun–Kyung et al. constructed an ultra-sensitive diagnostic platform called the trapLFI sensor (Figure 9c) [119]. The essential components of the trapLFI are according to typical competitive LFA sensors. As the antigen concentration increased, the signal in the detection zone was more prominent. The developed biosensor could detect cortisol ultra-sensitively. This platform can be used for daily monitoring of cortisol levels for stress state analysis.

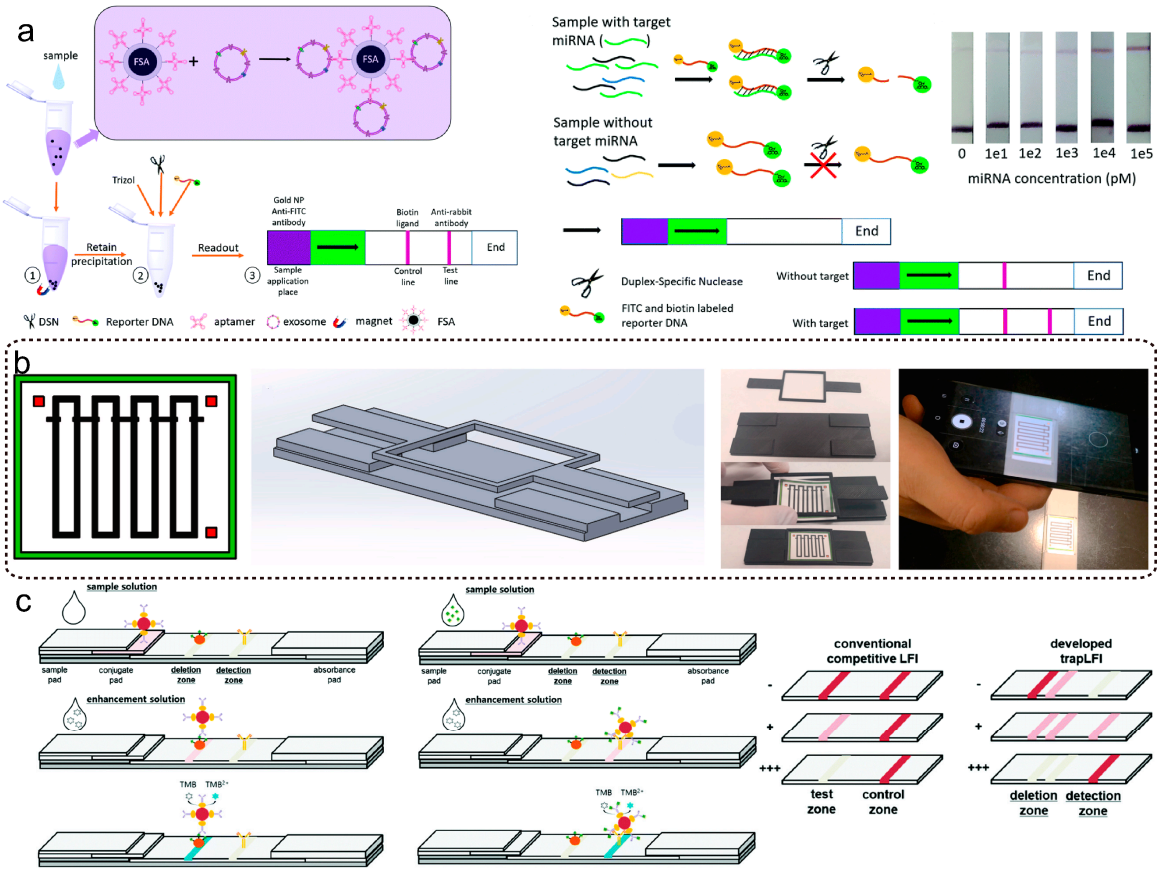

Figure 9. Potential applications of paper-based salivary sensors. (**a**) Schematics of the detection process (**left**); experimental design and results for the detection of miRNA (**right**). (Reproduced with permission from Ref. [114] Copyright 2020, Royal Society of Chemistry); (**b**) Flow profile assay of SARS-CoV-2 on a paper-based microfluidic chip. (Reproduced with permission from Ref. [116] Copyright 2022, Elsevier); (**c**) Schematic illustration of the mechanism of the developed trapLFI sensor with low and high concentrations of cortisol (**left**); signal tendency of the conventional and trapLFI with different concentrations of cortisol (**right**) (−: negative results; +: positive results +++: strong positive). (Reproduced with permission from Ref. [119] Copyright 2018, Royal Society of Chemistry).

Diabetes mellitus is a chronic metabolic syndrome that can lead to multiple complications. Glucose measurements are critical to the prevention and treatment of diabetes [120,121]. Santana–Jiménez et al. demonstrated a paper-based platform to detect glucose (Figure 10a) [122]. They used a stamping process to limit circular detection zones and modified it with chitosan to satisfy the best detection condition. Glucose was catalyzed by the GOx enzyme hydrogen peroxide (H_2O_2). Then the released H_2O_2 changed f4-APP/TBHBA chromophore from colorless to a purple-colored product. The device showed good performance as a semi-quantitative method. Wearable sensors have acquired extensive attention in recent decades. Particularly, there is a growing interest in developing various wearable health-monitor sensors, especially for people with reduced mobility [123]. For healthcare monitoring, wearable devices have been used to detect variable biomarkers. De Castro et al. first integrated µPADs into silicone mouthguards to develop paper-based wearable sensors (Figure 10b) [124]. Using a 3D-printed holder encloses the µPAD into the mouthguard for wearable paper-based devices. A colorimetric assay was carried out to detect glucose and nitrite., The nitrite concentrations were considerably higher for the periodontitis patients than for healthy. Moreover, diabetes and periodontitis have a two-way relationship, so monitoring both analytes may be helpful for a more complete diagnosis which is of paramount importance. This wearable device opens new horizons for paper-based platforms to produce simple, low-cost wearable sensors.

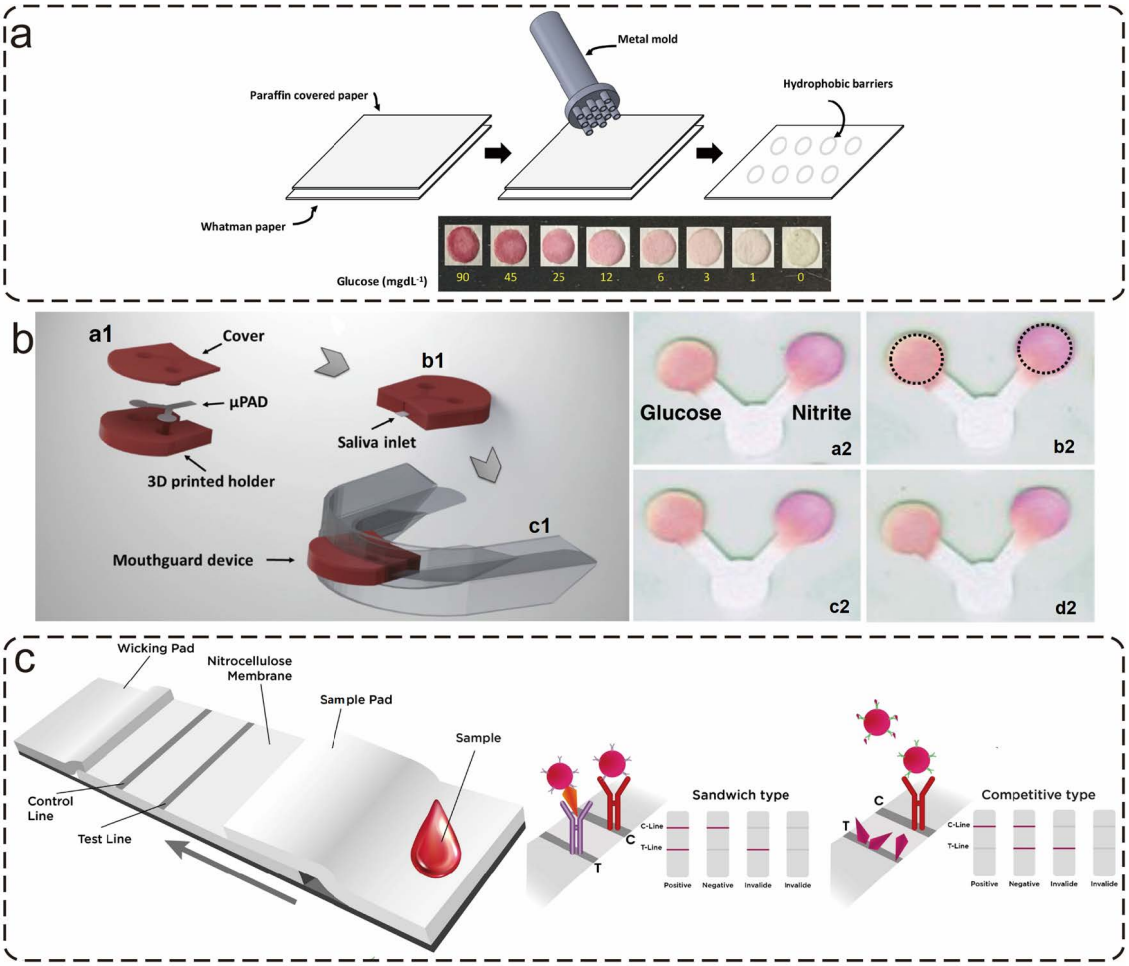

Figure 10. Salivary sensor for health monitoring or drug addiction detects. (**a**) Schematic of the paper-based sensor fabrication (**top**); naked-eye visual scale obtained for glucose detection (**bottom**). (Reproduced with permission from Ref. [122] Copyright 2018, MDPI); (**b**) The assembling of the μPAD into the mouthguard using a 3D-printed holder towards wearable paper-based devices, (**a1**–**c1**) indicate the insertion of the μPAD into the 3D-printed holder and the final device before and after integration into the mouthguard (**left**); simultaneous colorimetric assays for glucose and nitrite, (**a2**–**d2**) shows simultaneous colorimetric assays for glucose and nitrite in four different μPADs (**right**). (Reproduced with permission from Ref. [124] Copyright 2019, Springer Nature); (**c**) Illustration of the lateral flow assay system applied for the diagnosis of substance abuse and the results expected for positives and negatives with competitive or sandwich LFA formats. (Reproduced with permission from Ref. [50] Copyright 2021, Springer Nature).

4.3. Drug Addiction

Drug addiction (e.g., illegal drugs, nicotine, or alcohol) causes long-term severe harm to people's health. The increasing number of drug addicts annually places huge economic and public security burdens [125,126]. Many commercial sensors have been developed to detect illegal drugs, such as opioids. The effectiveness of commercially available LFIs designed to detect the synthetic opioid fentanyl in saliva has been evaluated by Daniel J. et al. [127]. Hichem et al. reported a colorimetric LFA sensor combined with a dye-loaded polymersome to efficiently detect the synthetic cannabinoid JWH-073 (Figure 10c) [50]. Rhodamine B is a dual-signal features dye (colorimetric and fluorescent). The Fluorescence of Rhodamine B was excited by a simple UV light. The sensitivity of the competitive LFA was successfully enhanced by the rhodamine B-loaded immunopolymersome. The LOD was 0.16 ng/mL.

While saliva is relatively easy to obtain noninvasively, it is worth considering that some addictive drugs can cause dry mouth, while food in the oral cavity may cause contamination. Intelligence device-based sensors detect could quantification of the results. It is wise to use machine learning algorithms to address these challenges. Liang et al. demonstrated a machine-learning platform for detecting cannabis [128]. They use a microfluidic competitive immunoassay and a smartphone-based fluorescence microscope to extract results and analyze them further. The classical classifications such as decision tree, k-nearest neighbor (k-NN), and support vector machine (SVM) have been developed to analyze the concentration of (−)-trans-Δ-tetrahydrocannabinol (THC) to eliminate salivary proteins interferences and individual variances, make this biosensor as a stable and reliable tool.

5. Challenges and Prospects

Paper-based saliva devices have flexible and convenient detection means, while some situations must be considered carefully and can be improved for the following generation of devices.

Though saliva is a powerful noninvasive detection method for diagnosing diseases, the optimal collecting saliva scheme has yet to be established. The whole saliva collection includes unstimulated whole saliva (USWS) and stimulated whole saliva (SWS) [31]. It has been proved that different saliva collection positions and methods impact the results. So, building standardized saliva collection steps allows the convenient collection of samples from patients and accurate diagnostic results.

Meanwhile, as a secreted bodily fluid, saliva is a complex mixed fluid with various constituents and physicochemical properties. Particularly the mucins, which make the largest contribution to the rheological properties of saliva. This particular viscosity of saliva makes researcher necessary to consider the driving force issues when designing the sensors. Vertical flow assay and micropump may be effective means, but more sophisticated designs need to be proposed to facilitate this problem [129].

Besides mucins, saliva contains proteins, epithelial cells, bacteria, and even food debris. However, the concentration of biomarkers in the saliva is lower than in serum. This is a great challenge for the sensitivity and specificity of the sensor. Pre-processing of the saliva, such as filtering and flushing, can reduce the interference but further reduce the concentration of biomarkers. These are the challenges that must be faced when detecting saliva biomarkers.

Additionally, their low cost means that paper-based sensors are mainly used as disposable detection devices. It is necessary to ensure consistency between the sensors. Industrialized mechanized production and consistent production steps are beneficial for the large-scale application of sensors.

It is undeniable that despite some aspects that should be considered in the design of paper-based saliva sensors, there is still a powerful noninvasive diagnostic tool. Currently, saliva sensors are evolving towards intelligent, all-purpose capabilities. For one thing, paper-based saliva sensor integration with smart and microelectronic devices and signal acquisition by camera make the detection more accurate. Algorithmic predictions facilitate a new form of interaction between humans and computers. For another, multiplexed sensor design enables simultaneous detection of various biomarkers, greatly reducing cost and time. Additionally, the new Internet of Things (IoT) has been steered toward an era of decentralized healthcare. Wearable sensors have enormous potential for point-of-care monitoring at home. Currently, many sensors have been developed for use in home medical care [130–135], and the combination of sensors and paper substrate will undoubtedly provide new avenues for health monitoring and preventive diagnostics.

6. Conclusions

This review aimed to build a design and application framework for paper-based saliva sensors and systematically introduced the types of sensors used for saliva detection in recent years, as well as application scenarios to highlight the need for sensor monitoring of

health status in this contemporary era. We further discussed in-depth challenges to remind interested researchers in these areas. We firmly believe that paper-based saliva sensors could change traditional healthcare models in the near future.

Author Contributions: C.C., Writing—original draft; L.T., Data curation and Validation; W.L., Validation; K.W., Investigation; Q.Y., Resources and Formal analysis; J.L., Software; T.Z.; Conceptualization; Supervision and Funding acquisition; B.D., Funding acquisition; L.W., Conceptualization; Supervision and Writing—review and editing. All authors have read and agreed to the published version of the manuscript.

Funding: This work was supported by the National Natural Science Foundation of China (82170998).

Institutional Review Board Statement: Not applicable.

Informed Consent Statement: Not applicable.

Data Availability Statement: Not applicable.

Acknowledgments: The author would like to thank Donghui Gao for the support in Conceptualization, Software and Project administration.

Conflicts of Interest: The authors declare no conflict of interest.

References

1. Siegel, R.L.; Miller, K.D.; Fuchs, H.E.; Jemal, A. Cancer Statistics, 2022. *CA Cancer J. Clin.* **2022**, *72*, 7–33. [CrossRef] [PubMed]
2. Chang, A.Y.; Skirbekk, V.F.; Tyrovolas, S.; Kassebaum, N.J.; Dieleman, J.L. Measuring Population Ageing: An Analysis of the Global Burden of Disease Study 2017. *Lancet Public Health* **2019**, *4*, e159–e167. [CrossRef]
3. Coronavirus Disease (COVID-19). Available online: https://www.who.int/emergencies/diseases/novel-coronavirus-2019/ (accessed on 2 February 2023).
4. Griesche, C.; Baeumner, A.J. Biosensors to Support Sustainable Agriculture and Food Safety. *TrAC Trends Anal. Chem.* **2020**, *128*, 115906. [CrossRef]
5. Hua, Z.; Yu, T.; Liu, D.; Xianyu, Y. Recent Advances in Gold Nanoparticles-Based Biosensors for Food Safety Detection. *Biosens. Bioelectron.* **2021**, *179*, 113076. [CrossRef] [PubMed]
6. Dai, Y.; Wu, Y.; Liu, G.; Gooding, J.J. CRISPR Mediated Biosensing Toward Understanding Cellular Biology and Point-of-Care Diagnosis. *Angew. Chem. Int. Ed.* **2020**, *59*, 20754–20766. [CrossRef] [PubMed]
7. Maduraiveeran, G.; Sasidharan, M.; Ganesan, V. Electrochemical Sensor and Biosensor Platforms Based on Advanced Nanomaterials for Biological and Biomedical Applications. *Biosens. Bioelectron.* **2018**, *103*, 113–129. [CrossRef]
8. Guo, M.; Wang, J.; Du, R.; Liu, Y.; Chi, J.; He, X.; Huang, K.; Luo, Y.; Xu, W. A Test Strip Platform Based on a Whole-Cell Microbial Biosensor for Simultaneous on-Site Detection of Total Inorganic Mercury Pollutants in Cosmetics without the Need for Predigestion. *Biosens. Bioelectron.* **2020**, *150*, 111899. [CrossRef]
9. Feng, Y.; Zhou, D.; Gao, L.; He, F. Electrochemical Biosensor for Rapid Detection of Bacteria Based on Facile Synthesis of Silver Wire across Electrodes. *Biosens. Bioelectron.* **2020**, *168*, 112527. [CrossRef]
10. Zhu, W.; Li, L.; Zhou, Z.; Yang, X.; Hao, N.; Guo, Y.; Wang, K. A Colorimetric Biosensor for Simultaneous Ochratoxin A and Aflatoxins B1 Detection in Agricultural Products. *Food Chem.* **2020**, *319*, 126544. [CrossRef]
11. Kundu, M.; Krishnan, P.; Kotnala, R.K.; Sumana, G. Recent Developments in Biosensors to Combat Agricultural Challenges and Their Future Prospects. *Trends Food Sci. Technol.* **2019**, *88*, 157–178. [CrossRef]
12. Sanvicens, N.; Mannelli, I.; Salvador, J.-P.; Valera, E.; Marco, M.-P. Biosensors for Pharmaceuticals Based on Novel Technology. *TrAC Trends Anal. Chem.* **2011**, *30*, 541–553. [CrossRef]
13. Qian, L.; Durairaj, S.; Prins, S.; Chen, A. Nanomaterial-Based Electrochemical Sensors and Biosensors for the Detection of Pharmaceutical Compounds. *Biosens. Bioelectron.* **2021**, *175*, 112836. [CrossRef] [PubMed]
14. Rebelo, R.; Barbosa, A.I.; Caballero, D.; Kwon, I.K.; Oliveira, J.M.; Kundu, S.C.; Reis, R.L.; Correlo, V.M. 3D Biosensors in Advanced Medical Diagnostics of High Mortality Diseases. *Biosens. Bioelectron.* **2019**, *130*, 20–39. [CrossRef]
15. Dervisevic, M.; Alba, M.; Prieto-Simon, B.; Voelcker, N.H. Skin in the Diagnostics Game: Wearable Biosensor Nano- and Microsystems for Medical Diagnostics. *Nano Today* **2020**, *30*, 100828. [CrossRef]
16. Chebil, A.; Mazzaracchio, V.; Cinti, S.; Arduini, F.; Dridi, C. Facile Development of Cost Effective and Greener for All Solid-State Supercapacitor on Paper Substrate. *J. Energy Storage* **2021**, *33*, 102107. [CrossRef]
17. Tai, W.-C.; Chang, Y.-C.; Chou, D.; Fu, L.-M. Lab-on-Paper Devices for Diagnosis of Human Diseases Using Urine Samples—A Review. *Biosensors* **2021**, *11*, 260. [CrossRef]
18. Nilghaz, A.; Guan, L.; Tan, W.; Shen, W. Advances of Paper-Based Microfluidics for Diagnostics—The Original Motivation and Current Status. *ACS Sens.* **2016**, *1*, 1382–1393. [CrossRef]

19. Mahato, K.; Srivastava, A.; Chandra, P. Paper Based Diagnostics for Personalized Health Care: Emerging Technologies and Commercial Aspects. *Biosensors and Bioelectronics* **2017**, *96*, 246–259. [CrossRef]
20. Kuswandi, B.; Ensafi, A.A. Perspective—Paper-Based Biosensors: Trending Topic in Clinical Diagnostics Developments and Commercialization. *J. Electrochem. Soc.* **2019**, *167*, 037509. [CrossRef]
21. Xia, Y.; Si, J.; Li, Z. Fabrication Techniques for Microfluidic Paper-Based Analytical Devices and Their Applications for Biological Testing: A Review. *Biosensors and Bioelectronics* **2016**, *77*, 774–789. [CrossRef]
22. Pan, X.; Li, L.; Lin, H.; Tan, J.; Wang, H.; Liao, M.; Chen, C.; Shan, B.; Chen, Y.; Li, M. A Graphene Oxide-Gold Nanostar Hybrid Based-Paper Biosensor for Label-Free SERS Detection of Serum Bilirubin for Diagnosis of Jaundice. *Biosens. Bioelectron.* **2019**, *145*, 111713. [CrossRef] [PubMed]
23. Adrover-Jaume, C.; Alba-Patiño, A.; Clemente, A.; Santopolo, G.; Vaquer, A.; Russell, S.M.; Barón, E.; González del Campo, M.d.M.; Ferrer, J.M.; Berman-Riu, M.; et al. Paper Biosensors for Detecting Elevated IL-6 Levels in Blood and Respiratory Samples from COVID-19 Patients. *Sens. Actuators B Chem.* **2021**, *330*, 129333. [CrossRef] [PubMed]
24. Zhang, J.; Liu, J.; Su, H.; Sun, F.; Lu, Z.; Su, A. A Wearable Self-Powered Biosensor System Integrated with Diaper for Detecting the Urine Glucose of Diabetic Patients. *Sens. Actuators B Chem.* **2021**, *341*, 130046. [CrossRef]
25. Tzianni, E.I.; Moutsios, I.; Moschovas, D.; Avgeropoulos, A.; Govaris, K.; Panagiotidis, L.; Prodromidis, M.I. Smartphone Paired SIM Card-Type Integrated Creatinine Biosensor. *Biosens. Bioelectron.* **2022**, *207*, 114204. [CrossRef] [PubMed]
26. Li, M.S.; Wong, H.L.; Ip, Y.L.; Peng, Z.; Yiu, R.; Yuan, H.; Wai Wong, J.K.; Chan, Y.K. Current and Future Perspectives on Microfluidic Tear Analytic Devices. *ACS Sens.* **2022**, *7*, 1300–1314. [CrossRef] [PubMed]
27. Sempionatto, J.R.; Brazaca, L.C.; García-Carmona, L.; Bolat, G.; Campbell, A.S.; Martin, A.; Tang, G.; Shah, R.; Mishra, R.K.; Kim, J.; et al. Eyeglasses-Based Tear Biosensing System: Non-Invasive Detection of Alcohol, Vitamins and Glucose. *Biosens. Bioelectron.* **2019**, *137*, 161–170. [CrossRef] [PubMed]
28. Borberg, E.; Granot, E.; Patolsky, F. Ultrafast One-Minute Electronic Detection of SARS-CoV-2 Infection by 3CLpro Enzymatic Activity in Untreated Saliva Samples. *Nat. Commun.* **2022**, *13*, 6375. [CrossRef]
29. Lomae, A.; Preechakasedkit, P.; Hanpanich, O.; Ozer, T.; Henry, C.S.; Maruyama, A.; Pasomsub, E.; Phuphuakrat, A.; Rengpipat, S.; Vilaivan, T.; et al. Label Free Electrochemical DNA Biosensor for COVID-19 Diagnosis. *Talanta* **2023**, *253*, 123992. [CrossRef]
30. Pedersen, A.M.L.; Sørensen, C.E.; Proctor, G.B.; Carpenter, G.H.; Ekström, J. Salivary Secretion in Health and Disease. *J. Oral. Rehabil.* **2018**, *45*, 730–746. [CrossRef]
31. Song, M.; Bai, H.; Zhang, P.; Zhou, X.; Ying, B. Promising Applications of Human-Derived Saliva Biomarker Testing in Clinical Diagnostics. *Int. J. Oral. Sci.* **2023**, *15*, 2. [CrossRef]
32. Zheng, X.; Zhang, F.; Wang, K.; Zhang, W.; Li, Y.; Sun, Y.; Sun, X.; Li, C.; Dong, B.; Wang, L.; et al. Smart Biosensors and Intelligent Devices for Salivary Biomarker Detection. *TrAC Trends Anal. Chem.* **2021**, *140*, 116281. [CrossRef]
33. Cui, Y.; Yang, M.; Zhu, J.; Zhang, H.; Duan, Z.; Wang, S.; Liao, Z.; Liu, W. Developments in Diagnostic Applications of Saliva in Human Organ Diseases. *Med. Nov. Technol. Devices* **2022**, *13*, 100115. [CrossRef]
34. Goldoni, R.; Farronato, M.; Connelly, S.T.; Tartaglia, G.M.; Yeo, W.-H. Recent Advances in Graphene-Based Nanobiosensors for Salivary Biomarker Detection. *Biosens. Bioelectron.* **2021**, *171*, 112723. [CrossRef] [PubMed]
35. Dong, T.; Matos Pires, N.M.; Yang, Z.; Jiang, Z. Advances in Electrochemical Biosensors Based on Nanomaterials for Protein Biomarker Detection in Saliva. *Adv. Sci.* **2022**, *10*, 2205429. [CrossRef]
36. Goldoni, R.; Dolci, C.; Boccalari, E.; Inchingolo, F.; Paghi, A.; Strambini, L.; Galimberti, D.; Tartaglia, G.M. Salivary Biomarkers of Neurodegenerative and Demyelinating Diseases and Biosensors for Their Detection. *Ageing Res. Rev.* **2022**, *76*, 101587. [CrossRef]
37. Tseng, C.-C.; Kung, C.-T.; Chen, R.-F.; Tsai, M.-H.; Chao, H.-R.; Wang, Y.-N.; Fu, L.-M. Recent Advances in Microfluidic Paper-Based Assay Devices for Diagnosis of Human Diseases Using Saliva, Tears and Sweat Samples. *Sens. Actuators B: Chem.* **2021**, *342*, 130078. [CrossRef]
38. Vyas, G.; Bhatt, S.; Si, M.K.; Jindani, S.; Suresh, E.; Ganguly, B.; Paul, P. Colorimetric Dual Sensor for Cu(II) and Tyrosine and Its Application as Paper Strips for Detection in Water and Human Saliva as Real Samples. *Spectrochim. Acta Part A Mol. Biomol. Spectrosc.* **2020**, *230*, 118052. [CrossRef]
39. Davidson, J.L.; Wang, J.; Maruthamuthu, M.K.; Dextre, A.; Pascual-Garrigos, A.; Mohan, S.; Putikam, S.V.S.; Osman, F.O.I.; McChesney, D.; Seville, J.; et al. A Paper-Based Colorimetric Molecular Test for SARS-CoV-2 in Saliva. *Biosens. Bioelectron. X* **2021**, *9*, 100076. [CrossRef]
40. Bahadır, E.B.; Sezgintürk, M.K. Lateral Flow Assays: Principles, Designs and Labels. *TrAC Trends Anal. Chem.* **2016**, *82*, 286–306. [CrossRef]
41. Grant, B.D.; Anderson, C.E.; Williford, J.R.; Alonzo, L.F.; Glukhova, V.A.; Boyle, D.S.; Weigl, B.H.; Nichols, K.P. SARS-CoV-2 Coronavirus Nucleocapsid Antigen-Detecting Half-Strip Lateral Flow Assay Toward the Development of Point of Care Tests Using Commercially Available Reagents. *Anal. Chem.* **2020**, *92*, 11305–11309. [CrossRef]
42. Nguyen, V.-T.; Song, S.; Park, S.; Joo, C. Recent Advances in High-Sensitivity Detection Methods for Paper-Based Lateral-Flow Assay. *Biosens. Bioelectron.* **2020**, *152*, 112015. [CrossRef]
43. Wang, N.; Zhang, J.; Xiao, B.; Sun, X.; Xie, R.; Chen, A. Recent Advances in the Rapid Detection of MicroRNA with Lateral Flow Assays. *Biosens. Bioelectron.* **2022**, *211*, 114345. [CrossRef]
44. Lin, J.T.; Saunders, D.L.; Meshnick, S.R. The Role of Submicroscopic Malaria in Malaria Transmission: What Is the Evidence? *Trends Parasitol.* **2014**, *30*, 183. [CrossRef]

45. Tao, D.; McGill, B.; Hamerly, T.; Kobayashi, T.; Khare, P.; Dziedzic, A.; Leski, T.; Holtz, A.; Shull, B.; Jedlicka, A.E.; et al. A Saliva-Based Rapid Test to Quantify the Infectious Subclinical Malaria Parasite Reservoir. *Sci. Transl. Med.* **2019**, *11*, eaan4479. [CrossRef] [PubMed]
46. Xie, Z.; Feng, S.; Pei, F.; Xia, M.; Hao, Q.; Liu, B.; Tong, Z.; Wang, J.; Lei, W.; Mu, X. Magnetic/Fluorescent Dual-Modal Lateral Flow Immunoassay Based on Multifunctional Nanobeads for Rapid and Accurate SARS-CoV-2 Nucleocapsid Protein Detection. *Anal. Chim. Acta* **2022**, *1233*, 340486. [CrossRef] [PubMed]
47. Pratt, G.W.; Fan, A.; Melakeberhan, B.; Klapperich, C.M. A Competitive Lateral Flow Assay for the Detection of Tenofovir. *Anal. Chim. Acta* **2018**, *1017*, 34–40. [CrossRef] [PubMed]
48. Panfilova, E. Development of a Prototype Lateral Flow Immunoassay of Cortisol in Saliva for Daily Monitoring of Stress. *Biosensors* **2021**, *11*, 146. [CrossRef]
49. Jung, C.; Kim, M.-G. Direct Use of a Saliva-Collected Cotton Swab in Lateral Flow Immunoassay for the Detection of Cotinine. *Biosensors* **2022**, *12*, 214. [CrossRef]
50. Moulahoum, H.; Ghorbanizamani, F.; Timur, S. Paper-Based Lateral Flow Assay Using Rhodamine B–Loaded Polymersomes for the Colorimetric Determination of Synthetic Cannabinoids in Saliva. *Microchim. Acta* **2021**, *188*, 402. [CrossRef]
51. Hu, Q.; Wei, Q.; Zhang, P.; Li, S.; Xue, L.; Yang, R.; Wang, C.; Zhou, L. An Up-Converting Phosphor Technology-Based Lateral Flow Assay for Point-of-Collection Detection of Morphine and Methamphetamine in Saliva. *Analyst* **2018**, *143*, 4646–4654. [CrossRef]
52. Cate, D.M.; Adkins, J.A.; Mettakoonpitak, J.; Henry, C.S. Recent Developments in Paper-Based Microfluidic Devices. *Anal. Chem.* **2015**, *87*, 19–41. [CrossRef] [PubMed]
53. Martinez, A.W.; Phillips, S.T.; Butte, M.J.; Whitesides, G.M. Patterned Paper as a Platform for Inexpensive, Low-Volume, Portable Bioassays. *Angew. Chem. Int. Ed.* **2007**, *46*, 1318–1320. [CrossRef] [PubMed]
54. Sriram, G.; Bhat, M.P.; Patil, P.; Uthappa, U.T.; Jung, H.-Y.; Altalhi, T.; Kumeria, T.; Aminabhavi, T.M.; Pai, R.K.; Madhuprasad; et al. Paper-Based Microfluidic Analytical Devices for Colorimetric Detection of Toxic Ions: A Review. *TrAC Trends Anal. Chem.* **2017**, *93*, 212–227. [CrossRef]
55. Asano, H.; Shiraishi, Y. Development of Paper-Based Microfluidic Analytical Device for Iron Assay Using Photomask Printed with 3D Printer for Fabrication of Hydrophilic and Hydrophobic Zones on Paper by Photolithography. *Anal. Chim. Acta* **2015**, *883*, 55–60. [CrossRef]
56. Taudte, R.V.; Beavis, A.; Wilson-Wilde, L.; Roux, C.; Doble, P.; Blanes, L. A Portable Explosive Detector Based on Fluorescence Quenching of Pyrene Deposited on Coloured Wax-Printed MPADs. *Lab. Chip* **2013**, *13*, 4164–4172. [CrossRef]
57. Guan, Y.; Sun, B. Detection and Extraction of Heavy Metal Ions Using Paper-Based Analytical Devices Fabricated via Atom Stamp Printing. *Microsyst. Nanoeng.* **2020**, *6*, 14. [CrossRef]
58. Cardoso, T.M.G.; de Souza, F.R.; Garcia, P.T.; Rabelo, D.; Henry, C.S.; Coltro, W.K.T. Versatile Fabrication of Paper-Based Microfluidic Devices with High Chemical Resistance Using Scholar Glue and Magnetic Masks. *Anal. Chim. Acta* **2017**, *974*, 63–68. [CrossRef]
59. Tong, X.; Lin, X.; Duan, N.; Wang, Z.; Wu, S. Laser-Printed Paper-Based Microfluidic Chip Based on a Multicolor Fluorescence Carbon Dot Biosensor for Visual Determination of Multiantibiotics in Aquatic Products. *ACS Sens.* **2022**, *7*, 3947–3955. [CrossRef]
60. Zhang, H.; Smith, E.; Zhang, W.; Zhou, A. Inkjet Printed Microfluidic Paper-Based Analytical Device (MPAD) for Glucose Colorimetric Detection in Artificial Urine. *Biomed. Microdevices* **2019**, *21*, 48. [CrossRef]
61. Assaifan, A.K.; Al Habis, N.; Ahmad, I.; Alshehri, N.A.; Alharbi, H.F. Scaling-up Medical Technologies Using Flexographic Printing. *Talanta* **2020**, *219*, 121236. [CrossRef]
62. Sousa, L.R.; Duarte, L.C.; Coltro, W.K.T. Instrument-Free Fabrication of Microfluidic Paper-Based Analytical Devices through 3D Pen Drawing. *Sens. Actuators B Chem.* **2020**, *312*, 128018. [CrossRef]
63. Chauhan, A.; Toley, B.J. Barrier-Free Microfluidic Paper Analytical Devices for Multiplex Colorimetric Detection of Analytes. *Anal. Chem.* **2021**, *93*, 8954–8961. [CrossRef] [PubMed]
64. Ferreira, F.T.S.M.; Mesquita, R.B.R.; Rangel, A.O.S.S. Novel Microfluidic Paper-Based Analytical Devices (MPADs) for the Determination of Nitrate and Nitrite in Human Saliva. *Talanta* **2020**, *219*, 121183. [CrossRef] [PubMed]
65. Jokerst, J.V.; Raamanathan, A.; Christodoulides, N.; Floriano, P.N.; Pollard, A.A.; Simmons, G.W.; Wong, J.; Gage, C.; Furmaga, W.B.; Redding, S.W.; et al. Nano-Bio-Chips for High Performance Multiplexed Protein Detection: Determinations of Cancer Biomarkers in Serum and Saliva Using Quantum Dot Bioconjugate Labels. *Biosens. Bioelectron.* **2009**, *24*, 3622–3629. [CrossRef]
66. Fabiani, L.; Mazzaracchio, V.; Moscone, D.; Fillo, S.; De Santis, R.; Monte, A.; Amatore, D.; Lista, F.; Arduini, F. Paper-Based Immunoassay Based on 96-Well Wax-Printed Paper Plate Combined with Magnetic Beads and Colorimetric Smartphone-Assisted Measure for Reliable Detection of SARS-CoV-2 in Saliva. *Biosens. Bioelectron.* **2022**, *200*, 113909. [CrossRef]
67. Fabiani, L.; Saroglia, M.; Galatà, G.; De Santis, R.; Fillo, S.; Luca, V.; Faggioni, G.; D'Amore, N.; Regalbuto, E.; Salvatori, P.; et al. Magnetic Beads Combined with Carbon Black-Based Screen-Printed Electrodes for COVID-19: A Reliable and Miniaturized Electrochemical Immunosensor for SARS-CoV-2 Detection in Saliva. *Biosens. Bioelectron.* **2021**, *171*, 112686. [CrossRef]
68. Xu, L.; Duan, J.; Chen, J.; Ding, S.; Cheng, W. Recent Advances in Rolling Circle Amplification-Based Biosensing Strategies-A Review. *Anal. Chim. Acta* **2021**, *1148*, 238187. [CrossRef]
69. Li, W.; Peng, W.; Zhang, Y.; Liu, P.; Gong, X.; Liu, H.; Chang, J. A Lateral Flow Strip Biosensor Platform Based on Cascade Nucleic Acid Amplification Technology for Ultrasensitive Detection of OSCC-Associated Salivary MicroRNA. *Anal. Chim. Acta* **2022**, *1221*, 340112. [CrossRef]

70. Varona, M.; Eitzmann, D.R.; Anderson, J.L. Sequence-Specific Detection of ORF1a, BRAF, and OmpW DNA Sequences with Loop Mediated Isothermal Amplification on Lateral Flow Immunoassay Strips Enabled by Molecular Beacons. *Anal. Chem.* **2021**, *93*, 4149–4153. [CrossRef]
71. Chen, J.S.; Ma, E.; Harrington, L.B.; Da Costa, M.; Tian, X.; Palefsky, J.M.; Doudna, J.A. CRISPR-Cas12a Target Binding Unleashes Indiscriminate Single-Stranded DNase Activity. *Science* **2018**, *360*, 436–439. [CrossRef]
72. Gootenberg, J.S.; Abudayyeh, O.O.; Lee, J.W.; Essletzbichler, P.; Dy, A.J.; Joung, J.; Verdine, V.; Donghia, N.; Daringer, N.M.; Freije, C.A.; et al. Nucleic Acid Detection with CRISPR-Cas13a/C2c2. *Science* **2017**, *356*, 438–442. [CrossRef] [PubMed]
73. Li, F.; Ye, Q.; Chen, M.; Zhou, B.; Zhang, J.; Pang, R.; Xue, L.; Wang, J.; Zeng, H.; Wu, S.; et al. An Ultrasensitive CRISPR/Cas12a Based Electrochemical Biosensor for Listeria Monocytogenes Detection. *Biosens. Bioelectron.* **2021**, *179*, 113073. [CrossRef] [PubMed]
74. Park, B.J.; Park, M.S.; Lee, J.M.; Song, Y.J. Specific Detection of Influenza A and B Viruses by CRISPR-Cas12a-Based Assay. *Biosensors* **2021**, *11*, 88. [CrossRef]
75. Chen, M.; Luo, R.; Li, S.; Li, H.; Qin, Y.; Zhou, D.; Liu, H.; Gong, X.; Chang, J. Paper-Based Strip for Ultrasensitive Detection of OSCC-Associated Salivary MicroRNA via CRISPR/Cas12a Coupling with IS-Primer Amplification Reaction. *Anal. Chem.* **2020**, *92*, 13336–13342. [CrossRef]
76. Fan, K.; Zeng, J.; Yang, C.; Wang, G.; Lian, K.; Zhou, X.; Deng, Y.; Liu, G. Digital Quantification Method for Sensitive Point-of-Care Detection of Salivary Uric Acid Using Smartphone-Assisted MPADs. *ACS Sens.* **2022**, *7*, 2049–2057. [CrossRef] [PubMed]
77. Mercan, Ö.B.; Kılıç, V.; Şen, M. Machine Learning-Based Colorimetric Determination of Glucose in Artificial Saliva with Different Reagents Using a Smartphone Coupled PAD. *Sens. Actuators B Chem.* **2021**, *329*, 129037. [CrossRef]
78. Liao, Z.; Zhang, Y.; Li, Y.; Miao, Y.; Gao, S.; Lin, F.; Deng, Y.; Geng, L. Microfluidic Chip Coupled with Optical Biosensors for Simultaneous Detection of Multiple Analytes: A Review. *Biosens. Bioelectron.* **2019**, *126*, 697–706. [CrossRef]
79. Gil Rosa, B.; Akingbade, O.E.; Guo, X.; Gonzalez-Macia, L.; Crone, M.A.; Cameron, L.P.; Freemont, P.; Choy, K.-L.; Güder, F.; Yeatman, E.; et al. Multiplexed Immunosensors for Point-of-Care Diagnostic Applications. *Biosens. Bioelectron.* **2022**, *203*, 114050. [CrossRef]
80. Pomili, T.; Donati, P.; Pompa, P.P. Paper-Based Multiplexed Colorimetric Device for the Simultaneous Detection of Salivary Biomarkers. *Biosensors* **2021**, *11*, 443. [CrossRef]
81. Shen, Y.; Modha, S.; Tsutsui, H.; Mulchandani, A. An Origami Electrical Biosensor for Multiplexed Analyte Detection in Body Fluids. *Biosens. Bioelectron.* **2021**, *171*, 112721. [CrossRef]
82. Liu, H.; Crooks, R.M. Three-Dimensional Paper Microfluidic Devices Assembled Using the Principles of Origami. *J. Am. Chem. Soc.* **2011**, *133*, 17564–17566. [CrossRef] [PubMed]
83. Fu, L.-M.; Wang, Y.-N. Detection Methods and Applications of Microfluidic Paper-Based Analytical Devices. *TrAC Trends Anal. Chem.* **2018**, *107*, 196–211. [CrossRef]
84. Bordbar, M.M.; Samadinia, H.; Sheini, A.; Aboonajmi, J.; Sharghi, H.; Hashemi, P.; Khoshsafar, H.; Ghanei, M.; Bagheri, H. A Colorimetric Electronic Tongue for Point-of-Care Detection of COVID-19 Using Salivary Metabolites. *Talanta* **2022**, *246*, 123537. [CrossRef] [PubMed]
85. Song, Y.; Wei, W.; Qu, X. Colorimetric Biosensing Using Smart Materials. *Adv. Mater.* **2011**, *23*, 4215–4236. [CrossRef]
86. Aldewachi, H.; Chalati, T.; Woodroofe, M.N.; Bricklebank, N.; Sharrack, B.; Gardiner, P. Gold Nanoparticle-Based Colorimetric Biosensors. *Nanoscale* **2018**, *10*, 18–33. [CrossRef]
87. Parolo, C.; Sena-Torralba, A.; Bergua, J.F.; Calucho, E.; Fuentes-Chust, C.; Hu, L.; Rivas, L.; Álvarez-Diduk, R.; Nguyen, E.P.; Cinti, S.; et al. Tutorial: Design and Fabrication of Nanoparticle-Based Lateral-Flow Immunoassays. *Nat. Protoc.* **2020**, *15*, 3788–3816. [CrossRef]
88. Oh, H.-K.; Kim, K.; Park, J.; Im, H.; Maher, S.; Kim, M.-G. Plasmon Color-Preserved Gold Nanoparticle Clusters for High Sensitivity Detection of SARS-CoV-2 Based on Lateral Flow Immunoassay. *Biosens. Bioelectron.* **2022**, *205*, 114094. [CrossRef]
89. Prainito, C.D.; Eshun, G.; Osonga, F.J.; Isika, D.; Centeno, C.; Sadik, O.A. Colorimetric Detection of the SARS-CoV-2 Virus (COVID-19) in Artificial Saliva Using Polydiacetylene Paper Strips. *Biosensors* **2022**, *12*, 804. [CrossRef]
90. Kim, H.; Awofeso, O.; Choi, S.; Jung, Y.; Bae, E. Colorimetric Analysis of Saliva–Alcohol Test Strips by Smartphone-Based Instruments Using Machine-Learning Algorithms. *Appl. Opt.* **2017**, *56*, 84. [CrossRef]
91. Hu, J.; Wang, S.; Wang, L.; Li, F.; Pingguan-Murphy, B.; Lu, T.J.; Xu, F. Advances in Paper-Based Point-of-Care Diagnostics. *Biosens. Bioelectron.* **2014**, *54*, 585–597. [CrossRef]
92. Sun, L.-J.; Xie, Y.; Yan, Y.-F.; Yang, H.; Gu, H.-Y.; Bao, N. Paper-Based Analytical Devices for Direct Electrochemical Detection of Free IAA and SA in Plant Samples with the Weight of Several Milligrams. *Sens. Actuators B Chem.* **2017**, *247*, 336–342. [CrossRef]
93. Ronkainen, N.J.; Halsall, H.B.; Heineman, W.R. Electrochemical Biosensors. *Chem. Soc. Rev.* **2010**, *39*, 1747–1763. [CrossRef] [PubMed]
94. Meirinho, S.G.; Dias, L.G.; Peres, A.M.; Rodrigues, L.R. Voltammetric Aptasensors for Protein Disease Biomarkers Detection: A Review. *Biotechnol. Adv.* **2016**, *34*, 941–953. [CrossRef] [PubMed]
95. Sivaranjanee, R.; Senthil Kumar, P.; Saravanan, R.; Govarthanan, M. Electrochemical Sensing System for the Analysis of Emerging Contaminants in Aquatic Environment: A Review. *Chemosphere* **2022**, *294*, 133779. [CrossRef]

96. Batista Deroco, P.; Giarola, J.d.F.; Wachholz Júnior, D.; Arantes Lorga, G.; Tatsuo Kubota, L. Chapter Four-Paper-Based Electrochemical Sensing Devices. In *Comprehensive Analytical Chemistry*; Merkoçi, A., Ed.; Paper Based Sensors; Elsevier: Amsterdam, The Netherlands, 2020; Volume 89, pp. 91–137.
97. Huang, X.; Shi, W.; Li, J.; Bao, N.; Yu, C.; Gu, H. Determination of Salivary Uric Acid by Using Poly(3,4-Ethylenedioxythipohene) and Graphene Oxide in a Disposable Paper-Based Analytical Device. *Anal. Chim. Acta* **2020**, *1103*, 75–83. [CrossRef] [PubMed]
98. Jaewjaroenwattana, J.; Phoolcharoen, W.; Pasomsub, E.; Teengam, P.; Chailapakul, O. Electrochemical Paper-Based Antigen Sensing Platform Using Plant-Derived Monoclonal Antibody for Detecting SARS-CoV-2. *Talanta* **2023**, *251*, 123783. [CrossRef]
99. Petruzzi, L.; Maier, T.; Ertl, P.; Hainberger, R. Quantitative Detection of C-Reactive Protein in Human Saliva Using an Electrochemical Lateral Flow Device. *Biosens. Bioelectron. X* **2022**, *10*, 100136. [CrossRef]
100. Li, Z.; Hou, J.-T.; Wang, S.; Zhu, L.; He, X.; Shen, J. Recent Advances of Luminescent Sensors for Iron and Copper: Platforms, Mechanisms, and Bio-Applications. *Coord. Chem. Rev.* **2022**, *469*, 214695. [CrossRef]
101. Roda, A.; Mirasoli, M.; Michelini, E.; Di Fusco, M.; Zangheri, M.; Cevenini, L.; Roda, B.; Simoni, P. Progress in Chemical Luminescence-Based Biosensors: A Critical Review. *Biosens. Bioelectron.* **2016**, *76*, 164–179. [CrossRef]
102. Roda, A.; Zangheri, M.; Calabria, D.; Mirasoli, M.; Caliceti, C.; Quintavalla, A.; Lombardo, M.; Trombini, C.; Simoni, P. A Simple Smartphone-Based Thermochemiluminescent Immunosensor for Valproic Acid Detection Using 1,2-Dioxetane Analogue-Doped Nanoparticles as a Label. *Sens. Actuators B Chem.* **2019**, *279*, 327–333. [CrossRef]
103. Yeh, H.-W.; Ai, H.-W. Development and Applications of Bioluminescent and Chemiluminescent Reporters and Biosensors. *Annu. Rev. Anal. Chem.* **2019**, *12*, 129–150. [CrossRef] [PubMed]
104. Hunt, J.P.; Zhao, E.L.; Free, T.J.; Soltani, M.; Warr, C.A.; Benedict, A.B.; Takahashi, M.K.; Griffitts, J.S.; Pitt, W.G.; Bundy, B.C. Towards Detection of SARS-CoV-2 RNA in Human Saliva: A Paper-Based Cell-Free Toehold Switch Biosensor with a Visual Bioluminescent Output. *New Biotechnol.* **2022**, *66*, 53–60. [CrossRef] [PubMed]
105. Wang, L.; Yan, R.; Huo, Z.; Wang, L.; Zeng, J.; Bao, J.; Wang, X.; Peng, Q.; Li, Y. Fluorescence Resonant Energy Transfer Biosensor Based on Upconversion-Luminescent Nanoparticles. *Angew. Chem. Int. Ed.* **2005**, *44*, 6054–6057. [CrossRef] [PubMed]
106. Chen, B.; Wang, F. Emerging Frontiers of Upconversion Nanoparticles. *Trends Chem.* **2020**, *2*, 427–439. [CrossRef]
107. Asghari, A.; Wang, C.; Yoo, K.M.; Rostamian, A.; Xu, X.; Shin, J.-D.; Dalir, H.; Chen, R.T. Fast, Accurate, Point-of-Care COVID-19 Pandemic Diagnosis Enabled through Advanced Lab-on-Chip Optical Biosensors: Opportunities and Challenges. *Appl. Phys. Rev.* **2021**, *8*, 031313. [CrossRef]
108. Juan-Colás, J.; Johnson, S.; Krauss, T.F. Dual-Mode Electro-Optical Techniques for Biosensing Applications: A Review. *Sensors* **2017**, *17*, 2047. [CrossRef]
109. Roda, A.; Cavalera, S.; Di Nardo, F.; Calabria, D.; Rosati, S.; Simoni, P.; Colitti, B.; Baggiani, C.; Roda, M.; Anfossi, L. Dual Lateral Flow Optical/Chemiluminescence Immunosensors for the Rapid Detection of Salivary and Serum IgA in Patients with COVID-19 Disease. *Biosens. Bioelectron.* **2021**, *172*, 112765. [CrossRef]
110. Bhardwaj, J.; Sharma, A.; Jang, J. Vertical Flow-Based Paper Immunosensor for Rapid Electrochemical and Colorimetric Detection of Influenza Virus Using a Different Pore Size Sample Pad. *Biosens. Bioelectron.* **2019**, *126*, 36–43. [CrossRef]
111. Pungjunun, K.; Yakoh, A.; Chaiyo, S.; Praphairaksit, N.; Siangproh, W.; Kalcher, K.; Chailapakul, O. Laser Engraved Microapillary Pump Paper-Based Microfluidic Device for Colorimetric and Electrochemical Detection of Salivary Thiocyanate. *Microchim. Acta* **2021**, *188*, 140. [CrossRef]
112. Tian, L.; Qian, K.; Qi, J.; Liu, Q.; Yao, C.; Song, W.; Wang, Y. Gold Nanoparticles Superlattices Assembly for Electrochemical Biosensor Detection of MicroRNA-21. *Biosens. Bioelectron.* **2018**, *99*, 564–570. [CrossRef]
113. Ngwa, W.; Addai, B.W.; Adewole, I.; Ainsworth, V.; Alaro, J.; Alatise, O.I.; Ali, Z.; Anderson, B.O.; Anorlu, R.; Avery, S.; et al. Cancer in Sub-Saharan Africa: A Lancet Oncology Commission. *Lancet Oncol.* **2022**, *23*, e251–e312. [CrossRef]
114. Zhou, P.; Lu, F.; Wang, J.; Wang, K.; Liu, B.; Li, N.; Tang, B. A Portable Point-of-Care Testing System to Diagnose Lung Cancer through the Detection of Exosomal MiRNA in Urine and Saliva. *Chem. Commun.* **2020**, *56*, 8968–8971. [CrossRef]
115. Ben Abdallah, S.; Mhalla, Y.; Trabelsi, I.; Sekma, A.; Youssef, R.; Bel Haj Ali, K.; Ben Soltane, H.; Yacoubi, H.; Msolli, M.A.; Stambouli, N.; et al. Twice-Daily Oral Zinc in the Treatment of Patients with Coronavirus Disease 2019: A Randomized Double-Blind Controlled Trial. *Clin. Infect. Dis.* **2023**, *76*, 185–191. [CrossRef] [PubMed]
116. Akarapipad, P.; Kaarj, K.; Breshears, L.E.; Sosnowski, K.; Baker, J.; Nguyen, B.T.; Eades, C.; Uhrlaub, J.L.; Quirk, G.; Nikolich-Žugich, J.; et al. Smartphone-Based Sensitive Detection of SARS-CoV-2 from Saline Gargle Samples via Flow Profile Analysis on a Paper Microfluidic Chip. *Biosens. Bioelectron.* **2022**, *207*, 114192. [CrossRef] [PubMed]
117. Devarakonda, S.; Singh, R.; Bhardwaj, J.; Jang, J. Cost-Effective and Handmade Paper-Based Immunosensing Device for Electrochemical Detection of Influenza Virus. *Sensors* **2017**, *17*, 2597. [CrossRef] [PubMed]
118. He, W.; You, M.; Li, Z.; Cao, L.; Xu, F.; Li, F.; Li, A. Upconversion Nanoparticles-Based Lateral Flow Immunoassay for Point-of-Care Diagnosis of Periodontitis. *Sens. Actuators B Chem.* **2021**, *334*, 129673. [CrossRef]
119. Oh, H.-K.; Kim, J.-W.; Kim, J.-M.; Kim, M.-G. High Sensitive and Broad-Range Detection of Cortisol in Human Saliva Using a Trap Lateral Flow Immunoassay (TrapLFI) Sensor. *Analyst* **2018**, *143*, 3883–3889. [CrossRef]
120. Zou, Y.; Chu, Z.; Guo, J.; Liu, S.; Ma, X.; Guo, J. Minimally Invasive Electrochemical Continuous Glucose Monitoring Sensors: Recent Progress and Perspective. *Biosens. Bioelectron.* **2023**, *225*, 115103. [CrossRef]
121. Danne, T.; Nimri, R.; Battelino, T.; Bergenstal, R.M.; Close, K.L.; DeVries, J.H.; Garg, S.; Heinemann, L.; Hirsch, I.; Amiel, S.A.; et al. International Consensus on Use of Continuous Glucose Monitoring. *Diabetes Care* **2017**, *40*, 1631–1640. [CrossRef]

122. Santana-Jiménez, L.; Márquez-Lucero, A.; Osuna, V.; Estrada-Moreno, I.; Dominguez, R. Naked-Eye Detection of Glucose in Saliva with Bienzymatic Paper-Based Sensor. *Sensors* **2018**, *18*, 1071. [CrossRef]
123. Yi, J.; Xianyu, Y. Gold Nanomaterials-Implemented Wearable Sensors for Healthcare Applications. *Adv. Funct. Mater.* **2022**, *32*, 2113012. [CrossRef]
124. De Castro, L.F.; de Freitas, S.V.; Duarte, L.C.; de Souza, J.A.C.; Paixão, T.R.L.C.; Coltro, W.K.T. Salivary Diagnostics on Paper Microfluidic Devices and Their Use as Wearable Sensors for Glucose Monitoring. *Anal. Bioanal. Chem.* **2019**, *411*, 4919–4928. [CrossRef] [PubMed]
125. Zhao, Y.; Qin, F.; Han, S.; Li, S.; Zhao, Y.; Wang, H.; Tian, J.; Cen, X. MicroRNAs in Drug Addiction: Current Status and Future Perspectives. *Pharmacol. Ther.* **2022**, *236*, 108215. [CrossRef] [PubMed]
126. Song, S.; Zilverstand, A.; Gui, W.; Pan, X.; Zhou, X. Reducing Craving and Consumption in Individuals with Drug Addiction, Obesity or Overeating through Neuromodulation Intervention: A Systematic Review and Meta-Analysis of Its Follow-up Effects. *Addiction* **2022**, *117*, 1242–1255. [CrossRef] [PubMed]
127. Angelini, D.J.; Biggs, T.D.; Maughan, M.N.; Feasel, M.G.; Sisco, E.; Sekowski, J.W. Evaluation of a Lateral Flow Immunoassay for the Detection of the Synthetic Opioid Fentanyl. *Forensic Sci. Int.* **2019**, *300*, 75–81. [CrossRef]
128. Liang, Y.; Zhou, A.; Yoon, J.-Y. Machine Learning-Based Quantification of (−)-*Trans*-Δ-Tetrahydrocannabinol from Human Saliva Samples on a Smartphone-Based Paper Microfluidic Platform. *ACS Omega* **2022**, *7*, 30064–30073. [CrossRef]
129. Nieuw Amerongen, A.V.; Ligtenberg, A.J.M.; Veerman, E.C.I. Implications for Diagnostics in the Biochemistry and Physiology of Saliva. *Ann. N. Y. Acad. Sci.* **2007**, *1098*, 1–6. [CrossRef]
130. Gao, W.; Emaminejad, S.; Nyein, H.Y.Y.; Challa, S.; Chen, K.; Peck, A.; Fahad, H.M.; Ota, H.; Shiraki, H.; Kiriya, D.; et al. Fully Integrated Wearable Sensor Arrays for Multiplexed in Situ Perspiration Analysis. *Nature* **2016**, *529*, 509–514. [CrossRef]
131. Zhang, H.; He, R.; Niu, Y.; Han, F.; Li, J.; Zhang, X.; Xu, F. Graphene-Enabled Wearable Sensors for Healthcare Monitoring. *Biosens. Bioelectron.* **2022**, *197*, 113777. [CrossRef]
132. Wang, J.; Wang, L.; Li, G.; Yan, D.; Liu, C.; Xu, T.; Zhang, X. Ultra-Small Wearable Flexible Biosensor for Continuous Sweat Analysis. *ACS Sens.* **2022**, *7*, 3102–3107. [CrossRef]
133. Zhao, T.; Fu, Y.; Sun, C.; Zhao, X.; Jiao, C.; Du, A.; Wang, Q.; Mao, Y.; Liu, B. Wearable Biosensors for Real-Time Sweat Analysis and Body Motion Capture Based on Stretchable Fiber-Based Triboelectric Nanogenerators. *Biosens. Bioelectron.* **2022**, *205*, 114115. [CrossRef] [PubMed]
134. Xu, J.; Tao, X.; Liu, X.; Yang, L. Wearable Eye Patch Biosensor for Noninvasive and Simultaneous Detection of Multiple Biomarkers in Human Tears. *Anal. Chem.* **2022**, *94*, 8659–8667. [CrossRef] [PubMed]
135. Zheng, H.; Han, X.; Wei, Q.; Liu, X.; Li, Y.; Zhou, J. A Green Flexible and Wearable Biosensor Based on Carbon Nanofibers for Sensitive Detection of Uric Acid in Artificial Urine. *J. Mater. Chem. B* **2022**, *10*, 8450–8461. [CrossRef] [PubMed]